C.P. No. 165
(15,548)
A.R.C. Technical Report



MINISTRY OF SUPPLY

AERONAUTICAL RESEARCH COUNCIL

CURRENT PAPERS

# A Theoretical Note on Effusion Cooled Gas Turbine Blades

By

R. Staniforth

LONDON HER MAJESTY'S STATIONERY OFFICE

1954

Price 4s 6d net

C.P. No. 165

# A theoretical note on effusion cooled gas turbine blades*

- by. -

R. Staniforth

## SUMMARY

Solutions of both dynamic and thermal boundary layer equations have been obtained for two dimensional isothermal incompressible laminar flow over semi-infinite wedges for a range of wedge angles and injection quantities. These solutions are applied to the estimation of cooling air injection velocity required by an effusion-cooled turbine blade, using an approximate method and also a method similar to that described by Eckert[1] and Mangler[2]. Proposals are given enabling calculated isothermal results to be applied to non-isothermal flow.

In the turbulent regime, a working hypothesis is given enabling the heat transfer coefficients and required cooling air velocity to be calculated, though the method must be regarded as tentative.

Details of the application of the theory are given in the main text whilst the full mathematical theory and methods of solution of the resulting equations are given in the Appendices.

The above treatment is applied to the design of two effusion cooled nozzle guide vanes for a high temperature gas turbine. In these designs, the "insulating" effect of the injected cooling air is such as to reduce the coefficient of heat transfer by about one-third as compared with the internally cooled case. The designs show the need for a great variation of cooling air injection velocity with chordwise position, if uniform cooling is to be achieved. The theory given in this memorandum cannot yet be checked by comparison with experiment, experimental data not being available.

An abridged version of this memorandum was presented at the General Discussion on Heat Transfer (London 1951)[3].

---

*"Effusion cooling" has been tentatively adopted at N.G.T.E. for cooling by injection of gas through a permeable wall: "sweat cooling" is being restricted to the injection of liquid through a permeable wall and "injection cooling" is being used as the generic term.

CONTENTS


| | | Page |
|---|---|---|
| 1.0 | Introduction | 5 |
| 2.0 | Theory of two dimensional, incompressible, isothermal, laminar flow over semi-infinite wedges with gas injection | 5 |
| 3.0 | Application of theory to blades with gas injection | 6 |
| 4.0 | Description of attached figures | 7 |
| 5.0 | Application to non-isothermal flow | 7 |
| 6.0 | Turbulent boundary layers with gas injection | 8 |
| 7.0 | Procedure for calculating the heat flow and required injection velocity consistent with maintaining a constant blade temperature | 8 |
| 8.0 | Design of an effusion cooled nozzle guide vane for a high temperature gas turbine | 11 |
| 9.0 | Comments on practicability of effusion cooling | 13 |
| 10.0 | Conclusions | 13 |
| References | | 14 |
| Bibliography | | 16 |


APPENDICES


| No. | Title | |
|---|---|---|
| I | List of symbols | 18 |
| II | Solution of the dynamic boundary layer equations | 21 |
| III | Note on the method of computing similar solutions of the boundary layer equations | 23 |
| IV | Solution of the thermal boundary layer equation | 26 |
| V | Note on porosity, permeability and pressure drop in sintered materials | 30 |

## ILLUSTRATIONS


| Fig. No. | Title |
|---|---|
| 1 | Solutions of isothermal boundary layer with gas injection $\beta = 0$ (flat plate). |
| 2 | Solutions of isothermal boundary layer with gas injection $\beta = 0.2$. |
| 3 | Solutions of isothermal boundary layer with gas injection $\beta = 0.5$. |
| 4 | Solutions of isothermal boundary layer with gas injection $\beta = 0.8$. |
| 5 | Solutions of isothermal boundary layer with gas injection $\beta = 1.0$ (stagnation point). |
| 6(a) | Dependence of the ratio $\frac{Nu_x}{\sqrt{Re_x}}$ upon injection and the pressure distribution. |
| 6(b) | Dependence of the function $\frac{1}{J(\infty)}$ upon injection and the pressure distribution. |
| 7 | Dependence of the momentum thickness $\Delta_2$ upon the pressure distribution and amount of injection. |
| 8 | Graph for the evaluation of the quantity $Zt^{*2}$ from the form parameter $\lambda t^*$ and the injection parameter C. |
| 9 | Graph for the evaluation of the quantity $Zt^{*2}$ from the form parameter $\lambda t^*$ and the temperature parameter. |
| 10 | Graph for the evaluation of the injection parameter C for a given wedge angle ($\beta$) and temperature parameter. |
| 11(a) | Details of W2/700 nozzle guide vane cascade. |
| 11(b) | Velocity distribution over the surface of the W2/700 nozzle guide vane. |
| 12 | Graph of $\frac{\delta t^*}{s_{1,2}}\sqrt{Re_s}$ against $\frac{x}{s_{1,2}}$ for the W2/700 nozzle guide vane with no injection. |
| 13 | Graph of $\frac{\delta t^*}{s_{1,2}}\sqrt{Re_s}$ against $\frac{x}{s_{1,2}}$ for the W2/700 nozzle guide vane effusion cooled to 600°C. |
| 14(a) | Cooling air velocity distribution required to cool a nozzle guide vane to 600°C. in a gas stream at 1,000°C. (approximate solution). |

ILLUSTRATIONS (Cont'd.)


| Fig. No. | Title |
|---|---|
| 14(b) | Comparison of heat transfer with and without injection (approximately solution). |
| 15(a) | Cooling air velocity distribution required to cool a nozzle guide vane to 600°C. in a gas stream at 1,000°C. |
| 15(b) | Comparison of heat transfer with and without injection. |
| 16 | Relative wall thickness of an effusion cooled nozzle guide vane. |
| 17(a) | Details of a nozzle cascade |
| 17(b) | Velocity distribution over the surface of a nozzle blade. |
| 18(a) | Cooling air velocity required to cool a nozzle blade to 600°C. in a gas stream at 1,200°C. Re = $2 \times 10^5$. |
| 18(b) | Comparison of heat transfer with and without injection. |
| 19 | Relative wall thickness of an effusion cooled nozzle blade. |

## 1.0 Introduction

Because of the complex nature of the equations governing the boundary layer, it is impossible with our present knowledge to obtain a mathematically exact solution to the aerodynamic design problems of effusion cooled blades. We are therefore obliged to seek an approximate method or an empirical method. As no accurate experimental data concerning this problem have been published, the latter course cannot be explored.

It has been shown[4] that exact solutions of the isothermal boundary layer equations can be obtained for flow over semi-infinite wedges and flow through certain kinds of channels without fluid injection. As fluid injection and abstraction alters in no way the mathematical reasoning leading to the above conclusion, we can obtain a range of corresponding solutions with injection and abstraction, a special case of which, with no injection, being the solution usually quoted.

It is proposed to apply these solutions to a body of more complex shape such as a turbine blade by approximating the velocity distribution over its surface to either a single wedge or a series of wedges.

## 2.0 Theory of two dimensional, incompressible, isothermal laminar flow over semi-infinite wedges with gas injection

For flow over a semi-infinite wedge, the boundary layer equations resolve to a non-linear total differential equation[5].

$$f'''(\eta) + f(\eta)\, f''(\eta) = \beta \left\{ f'(\eta)^2 - 1 \right\} \quad .. \quad .. \quad .. \qquad (1)$$

with boundary conditions

$$\eta = 0, \; f'(\eta) = 0, \; f(\eta) = C$$

$$\eta \to \infty, \; f'(\eta) = 1$$

and where $\eta$ is the non-dimensional distance normal to the surface and $f'(\eta)$ is the dimensionless velocity parallel to the surface (see Appendix I for list of symbols).

For completeness a development of this equation from the boundary layer equations is given in Appendix II. Several solutions of this equation have been published,[6],[7],[8],[9] and further solutions required were calculated by the method outlined by I. Fox[10] (see Appendix III).

The temperature boundary layer solution can be computed from the following equations knowing the values of $f(\eta)$.

$$\theta = \frac{J(\eta)}{J(\infty)}, \; J(\eta) = \int_0^{\eta} e^{-F(\eta)}\, d\eta, \; F(\eta) = Pr \int_0^{\eta} f(\eta)\, d\eta, \; \theta = \frac{T - T_b}{T_g - T_b} \quad .. \qquad (2)$$

Appendix IV shows the derivation of the above solution. Further mathematical manipulation required to convert the solutions into a more practicable form is also included in this Appendix.

Some known solutions of equation 1 are shown graphically in Figures 1 to 5 for a Prandtl number = 0.71. Other characteristics of the boundary layer, namely $\frac{Nu_x}{\sqrt{Re_x}}$, $\frac{1}{J(\infty)}$ and $\Delta_2$, the momentum thickness were calculated and are plotted in Figures 6 and 7. From these graphs, the dependence of the boundary layer thickness and the heat transfer coefficient upon the pressure distribution and injection coefficient can be clearly seen.

## 3.0 Application of theory to blades with gas injection

Two methods of application of the above results to the solution of any blade design problem may be used, the one chosen depending upon the accuracy desired. The simplest is to replace the given velocity distribution over the blade surface by a single curve corresponding to the flow over a semi-infinite wedge. The choice of wedge angle may be made by trial and error or by plotting the velocity profile on logarithmic axes and determining the average slope of the graph. This gives $m = \frac{\beta}{2-\beta}$ which is the parameter governing the wedge angle. If we require the body to be cooled to a uniform temperature, the injection parameter C is constant (because in Appendix IV equation 10, $J(\infty)$ is independent of x) and therefore we know immediately the velocity of injection at any point, and the local heat transfer coefficients.

This approximation leads to the largest error at the leading edge although this can be reduced by calculating the exact heat transfer and injection quantities at the nose as in Section 7 and fairing in the curves to include this point.

A second and more accurate method, suggested by several writers, is to split up the profile into a large number of sections and fit a wedge velocity distribution to each piece. The sections are joined together by assuming the continuity of a function of the boundary layer. As it is impossible for one parameter to describe fully all the characteristics of a boundary layer, there remains the choice of a parameter which, as well as agreeing with other methods and experiments, is also convenient to use. The parameters usually adopted are the boundary layer thicknesses of which the following are the four most common:-

1. Displacement thickness $\delta^*$
2. Momentum thickness $\Delta_2$
3. Nominal thickness
4. Temperature displacement thickness $\delta t^*$

The first two functions are inconvenient to use for the subject of this note as the relation $Z^{*2}$ to $\lambda^*$ is ambiguous for high values of $\beta$. ($Z^{*2}$ and $\lambda^*$ are functions of the dynamic boundary layer corresponding to $Z_t^{*2}$ and $\lambda_t^*$ in the temperature boundary layer).

The temperature displacement thickness has been used below although no doubt the nominal boundary layer thickness would be just as suitable.

In this analysis described in more detail in Section 7.1, we proceed to draw a graph of the dimensionless temperature displacement thickness $\frac{\delta t^*}{s}\sqrt{Re_s}$ against the distance $^x/_s$ from the blade stagnation point, using the isocline method. Equations 8 and 9, Appendix IV, are particularly suitable for solution by the isocline method, as at any point on the graph, i.e., knowing $\frac{\delta t^*}{s}\sqrt{Re_s}$ and $\frac{d\,(U/U_0)}{d\,^x/_s}$ we can calculate the function of $\lambda t^*$ from Equation 8, Appendix IV. From a chart, described later (Figure 9), we can obtain the value of $(1-\beta)\,Zt^{*2}$ enabling $\frac{d\,(\delta t^*/_s\ \sqrt{Re_s})}{d\,(^x/_s)}$ to be obtained (Equation 9, Appendix IV). Thus we may plot a series of short lines through selected values of $\frac{\delta t^*}{s}\sqrt{Re_s}$ at each $^x/_s$ station (the positions of these should of course be carefully estimated), each line being at the slope predicted.

As the initial value of $\frac{\delta t^*}{s}\sqrt{Re_s}$ at the stagnation point ($\beta = 1$) is known from Equation 8, Appendix IV, and as the slope there is known to be zero, we can sketch the most probable path of the curve (see Figure 12, no injection, Figure 13 with injection).

## 4.0 Description of attached figures

The most convenient co-ordinates for obtaining the function $(1-\beta)\,Zt^{*2}$ are $\lambda t^*$ and $Zt^{*2}$, the difference between the co-ordinates being the desired function and the inverse slope being $\beta$. The calculated values of the above co-ordinates were plotted and graphed, the parameter being C (Figure 8). The injection parameter C is difficult to evaluate at any point except by trial and error because it is a function of x, the origin of which is usually unknown. The parameter is therefore changed using Equation 10, Appendix IV, and the graph re-plotted with the temperature ratio as a parameter (Figure 9). Other parameters could be employed but they suffer from a disadvantage in that they have singular points.

## 5.0 Application to non-isothermal flow

There are two methods in general use for co-relating non-isothermal and isothermal heat transfer coefficients. One method is to choose the temperatures at which the physical data are taken such that the relationship $\frac{Nu}{\sqrt{Re}}$ can be independent of the blade-gas absolute temperature ratio. Alternatively, the relation $\frac{Nu}{\sqrt{Re}}$ can be calculated using free stream conditions and a correction factor introduced which is a function of the blade-gas absolute temperature ratio.

If the first method were used, the relevant values of the physical data used for the calculation of the injection parameter C would be the subject of pure speculation. Rather than adopt this practice, it was decided to adopt the second process, first determining the heat transfer coefficient for isothermal flow at the main stream temperature, correcting only for the change in $C_p$ of the cooling fluid and then applying this heat transfer coefficient to the non-isothermal case with a suitable correction for the absolute temperature ratio.

This procedure leads us to a modified value for the temperature parameter

$$= \frac{(T_b - T_c)}{(T_g - T_b)} \; \frac{C_{p\,b.c.}}{C_{p_g}} \, Pr \qquad \ldots \quad \ldots \quad \ldots \quad \ldots \quad \ldots \qquad (3)$$

Heat transfer coefficients and cooling air mass flows are modified by a factor depending on the ratio $\frac{T_b}{T_g}$, the value of this function being taken as

$$f\left(\frac{T_b}{T_g}\right) = 0.7 + 0.3\left(\frac{T_b}{T_g}\right) \qquad \ldots \quad \ldots \quad \ldots \quad \ldots \quad \ldots \quad \ldots \qquad (4)$$

for $0.5 < \frac{T_b}{T_g} < 1$. This equation must be considered approximate as it is deduced from only one set of experimental data[11].

## 6.0 Turbulent boundary layers with gas injection

At present, nothing is known regarding the behaviour of an undeveloped turbulent boundary layer when a gas is injected at the wall with regard to modification of its velocity profile, thickness, and heat transfer, although a little information is available on the heat transfer to the wall of a porous tube with undeveloped turbulent flow[12]. It appears that the Nusselt number is reduced only a small amount by air injection. We could therefore expect that the heat transfer in the turbulent regime of the blade would be somewhat less than that calculated for no injection; the actual fraction depends on the amount of injected air. It is suggested that the coefficients should be calculated on a basis that there is no injection in the turbulent region using Young's method[13],[14]. This is probably an over-estimate of the coolant required for various reasons and should be modified as experimental data becomes available.

It should be noted that Young's method postulates sudden transition to turbulence whereas in practice it is found that transition takes a finite distance to complete.

## 7.0 Procedure for calculating the heat flow and required injection velocity consistent with maintaining a constant blade temperature

In order to calculate the boundary layer thickness and heat transfer coefficients, it is first essential to obtain accurately the potential velocity distribution over the blade surface by either experiment, calculation or electrical analogy. From these results $U/U_o$ and $\frac{d\,U/U_o}{d^x/_s}$ are tabulated at close regular intervals.

At the nose $\frac{d\,U/U_o}{d^x/_s}$ is calculated from the nose curvature using the following equation derived from elementary potential flow theory:

$$\frac{d\,U/U_o}{d^x/_s} = 2\,\frac{s}{R}\;\frac{U\ in}{U\ out} \qquad \text{.. .. .. .. ..} \qquad (5)$$

the ratio $\frac{U\ in}{U\ out}$ being calculated from the blade angles assuming incompressible flow.

7.1 <u>Procedure</u>

(1) Given $T_b$, $T_c$, and $T_g$ calculate the ratio $\frac{(T_b - T_c)\ C_{p_{b,\,c}}}{(T_g - T_b)\ C_{p_g}}\,Pr$

(2) At the stagnation point where $\beta = 1$, we can obtain the function $\lambda t^*$ using Figure 9 and the temperature ratio calculated above.

This enables us to determine $\frac{\delta t^*}{s}\sqrt{Re_s}$ at this point by the use of Equation 8, Appendix IV. We then proceed to complete the curve as described at the end of Section 3.0 (using the method of isoclines) over the whole of the concave surface and up to the point of maximum velocity (or minimum pressure) on the convex surface.

We then tabulate the values of $\frac{\delta t^*}{s}\sqrt{Re_s}$ at the chosen points, and proceed to calculate $\frac{Nu}{\sqrt{Re}}$ and $\frac{q}{Q}\sqrt{Re}$ as in Table I:-

TABLE I

| $\frac{\delta t^*}{s}\sqrt{Re_s}$ | $\frac{d\,U/U_o}{d\,x/s}$ | $\lambda t^*$ | $Zt^{*2}$ | $\beta$ | C | $\frac{q}{Q}\sqrt{Re}$ | $\frac{Nu}{\sqrt{Re}}$ |
|---|---|---|---|---|---|---|---|
| From graph Fig. 13 | Known | $\left(\frac{\delta t^*}{s}\sqrt{Re_s}\right)^2 \frac{d\,U/U_o}{d\,x/s}$ (Equation 8 Appendix IV) | From Fig.9 | $=\frac{\lambda t^*}{Zt^{*2}}$ | Fig.8 or 10 | $=-f\left(\frac{T_b}{T_g}\right) \frac{C\,Zt^*}{\delta t^*/s\,\sqrt{Re_s}}\sqrt{\frac{c}{s}}$ (Equation 11a Appendix IV) | $=\left\{\frac{(T_b - T_c)}{(T_g - T_b)}\frac{c_{p_{b,c}}}{c_{pg}}Pr\right\}\cdot\frac{q}{Q}\sqrt{Re}$ (Equation 12a Appendix IV) |

The point of transition to turbulence on the convex surface is assumed to be the point of maximum velocity or minimum pressure. We can then calculate the momentum thickness of the laminar boundary layer at this point as follows:-

$$\frac{\theta}{s}\ Re_s = \frac{\delta t^*}{s}\sqrt{Re_s}\ \frac{\Delta 2}{Zt^*}\sqrt{Re_s} \quad \ldots \quad \ldots \quad \ldots \quad \ldots \quad \ldots \quad (6)$$

$\Delta_2$ being read from graph 7. The heat transfer coefficients in the turbulent region are now calculated as in References 13 and 14.

As before

$$\frac{Nu}{\sqrt{Re}} = f_1\left(\frac{T_b}{T_g}\right)\left[\frac{Nu}{\sqrt{Re}}\right]_{isothermal} \qquad \frac{q}{Q}\sqrt{Re} = \frac{Nu}{\sqrt{Re}}\left\{\frac{(T_b - T_c)}{(T_g - T_b)}\ \frac{C_{Pb,c}}{C_{Pg}}\ Pr\right\}^{-1}$$

$$\ldots \quad \ldots \quad \ldots \quad (7)$$

The value of the function $f_1\left(\frac{T_b}{T_g}\right)$ is unknown. It is therefore assumed that this function is the same as that used in the laminar flow case.

## 8.0 Design of an effusion cooled nozzle guide vane for a high temperature gas turbine

As the blade under consideration is subject to turbulent flow as well as laminar, it is difficult to maintain a constant blade temperature under all operating Reynolds numbers.

The blade must be designed at the worst estimated conditions so that under other more favourable conditions, the blade will be over cooled. The potential velocity distribution over the surface of the W2/700 nozzle guide vane cascade, the first example taken, together with relevant physical dimensions, are given in Figure 11.

As further design data is unavailable concerning the example given, it has been assumed that the design condition is Re = 2 x $10^5$.

The pressure distribution round the blade was obtained assuming the flow to be incompressible. The outstanding design figures are tabulated below:-

| | | | | | |
|---|---|---|---|---|---|
| Equivalent gas temperature at exit ($T_g$ + 0.86 $\theta_v$) | | | | | 1,000°C. |
| Total | " | " | " | " | 1,012°C. |
| Static | " | " | " | " | 927°C. |
| Coolant temperature | | | | | 60°C. |
| Maximum blade temperature | | | | | 600°C. |

| | |
|---|---|
| Static pressure at exit | 25 lb./sq. in. gauge |
| Cooling air pressure | 40 lb./sq. in. gauge |
| Exit gas velocity | 1,465 f.p.s. |
| Temperature parameter | 0.86 |

The required solution of the boundary layer equations has already been obtained (Figure 13).

If the blade material is of constant permeability and if the pressure distribution, internal pressure and the injection velocity profile are known, the relative wall thicknesses can readily be calculated (Figure 16).

The scale of this graph is dependent upon the permeability of the blade material.

With a permeability of $5 \times 10^{-10}$ in.$^2$, the required thickness at the stagnation point is approximately 0.004 in. giving a maximum blade thickness of 0.077 in. It may be necessary to increase the wall thickness at the nose to ease stressing and manufacturing difficulties. This may be achieved by using a larger blade nose radius, a higher coolant pressure, or by allowing the nose temperature to rise above that in the specification.

Alternatively, the wall can be made of a material of variable permeability using a constant blade wall thickness.

The percentage cooling air required is dependent upon the Reynolds number, the calculated figures being 1.22 per cent at Re = $5 \times 10^5$ and 1.71 per cent at Re = $2 \times 10^5$.

These figures are higher than would be usual in gas turbine practice because of the close spacing of the blades.

This process was repeated for a similar type of blade of much greater thickness(15) as it was considered that the first blade, which was designed for an uncooled turbine, was unsuitable for this method of cooling.

The relevant design data is as follows:-

| | |
|---|---|
| Design Reynolds number | $2 \times 10^5$ |
| Equivalent gas temperature at exit ($T_g + 0.86\ \theta_v$) | 1,200°C. |
| Total " " " " | 1,207°C. |
| Static " " " " | 1,159°C. |
| Coolant temperature | 60°C. |
| Maximum blade temperature | 600°C. |
| Static pressure at exit | 28.4 lb./sq. in. gauge |
| Cooling air pressure | 54 lb./sq. in. gauge |
| Temperature parameter | 0.555 |

The corresponding figures are Figures 17, 18 and 19.

The cooling air quantity required to effusion cool the blade is 1.12 per cent and the quantity of air to indirectly cool the blade at 100 per cent cooling efficiency is 1.56 per cent. In Figure 19, the units of wall thickness are 0.004 in., for a material of the same permeability as mentioned previously.

## 9.0 Comments on practicability of effusion cooling

It can be seen by reference to Figure 16 that it would be difficult to manufacture such a blade with thin sections as are required at the leading and trailing edges.

A great deal could be done in alleviating the design problems in a high temperature turbine blade, directly cooled or sweat cooled, by investigation into unorthodox blades of relatively large thickness with a view to their use in similar designs to the above.

In cooling a blade directly by injecting cooling air through the blade walls, the heat transferred from the gas to the blade walls is only about $^2/_3$ of that transferred to a blade at the same temperature but internally cooled. The saving of cooling air would probably be greater than $^1/_3$ because of the difficulty in obtaining sufficient heat transfer in the blade using indirect methods to enable the cooling air to be efficiently used.

Providing care is taken in filtering the cooling air, trouble due to overheating of the blade arising from blocking of the pores of the metal with foreign matter should not cause any difficulty.

## 10.0 Conclusions

A process has been outlined for the thermal design of an effusion cooled gas turbine blade such as would be employed in a high temperature gas turbine.

## Acknowledgment

To Miss M. G. Kennard for the calculations of the solutions of Equation 8, Appendix II, on which this work is based.

## REFERENCES


| No. | Author(s) | Title |
| --- | --- | --- |
| 1 | E. Eckert | Die Berechnung des Wärmeüberganges in der laminaren Grenzschicht umströmter Körper. V.D.I. Forschungscheft No.416. Berlin 1942. |
| 2 | W. Mangler | Boundary Layers: approximate methods. R. & T. 1002, GDC/3235.T. |
| 3 | R. Staniforth | Contribution to the theory of effusion cooling of gas turbine blades. General Discussion of Heat Transfer, Section V - Special Problems. London Conference at the Institute of Mechanical Engineers 11-13th September 1951. |
| 4 | W. Mangler | Boundary layers: Steady laminar boundary layers: Special exact solutions. M.A.P. Volkenrode AVA Monograph. R. & T. 1001, GDC/3234.T. |
| 5 | S. Goldstein (Editor) | Modern developments in fluid dynamics. Camb. Univ. Press (1938), p.141. |
| 6 | H. Schlichting and K. Bussmann | Exakte Lösungen für die laminare Grenzschicht mit Absaugung und Ausblasen. Schriften der Deutschen Akademie der Luftfahrtforschung. 7B (1943), Vol.2. |
| 7 | M. Schaefer | Laminar boundary layer for the potential flow $U = U_1 x^m$ with suction and blowing. U.M.2043 (1944). |
| 8 | W. Mangler | Laminar boundary layer with suction and blowing. U.M.3087 (1944). |
| 9 | H. Holstein | Similar laminar boundary layers at permeable walls. U.M.3050 (1943). |
| 10 | L. Fox | The solution by relaxation methods of ordinary differential equations. Proc. Camb. Phil. Soc. Vol.45, Part I. January 1949, p.50. |
| 11 | S. J. Andrews and P. C. Bradley | Heat transfer to turbine blades. N.G.T.E. Memorandum No. M.37. A.R.C. 12,078. October, 1948. |
| 12 | P. Duwez and H. L. Wheeler | Experimental study of cooling by infiltration of a fluid through a porous material. Journal of the Aeronautical Sciences, Vol.15, No.9. September 1948, p.508. |
| 13 | H. B. Squire | Heat transfer calculation for aerofoils. A.R.C. R. & M. 1986. November (1942). |

REFERENCES (Cont'd.)


| No. | Author(s) | Title |
| --- | --- | --- |
| 14 | H. B. Squire and A. D. Young | The calculation of the profile drag of aerofoils. A.R.C. R. & M. 1838. November 1937. |
| 15 | S. J. Andrews and N. W. Schofield | An experimental investigation of a thick aerofoil nozzle cascade. N.G.T.E. Memorandum No. M.84. A.R.C. 13632. May 1950. |
| 16 | R. V. Southwell | Relaxation methods. Clarendon Press (1946). |

## BIBLIOGRAPHY


Author(s)

Experimental investigations

"Cooling by forcing a fluid through a porous plate in contact with a hot gas stream". Presented at the Heat Transfer and Fluid Mechanics Institute. Published by A.S.M.E., May, 1949. — M. Jakob and I. B. Fieldhouse

"Heat transfer measurements in a nitrogen sweat cooled porous tube". Progress Report 4-48: Pasadena, Jet Propulsion Laboratory, 6th November, 1947. — P. Duwez and H. L. Wheeler

"Experimental study of cooling by infiltration of a fluid through a porous metal". VIth International Congress for Applied Mechanics. Paris, September, 1946. — P. Duwez

"Heat transfer to a porous wall through which a gas is injected". VIIth International Congress for Applied Mechanics. London, September, 1948. — P. Duwez and H. L. Wheeler

"The powder metallurgy of porous metals and alloys having a controlled porosity". A.I.M.E. Tech. Pub. 2343, 1948. — P. Duwez and H. E. Martens

Theoretical investigations

"The flow of gases through porous metal compacts". "Engineering", Vol.167, No.434, April, 1949, pp.291-292. — P. Grootenhuis

"An empirical equation for heat transfer in a tube sweat-cooled with a gas". Progress Report No.4-49, Pasadena, Jet Propulsion Laboratory, 19th November, 1947. — H. L. Wheeler

"A simplified theory of porous wall cooling". Progress Report No.4-50: Pasadena, Jet Propulsion Laboratory, 24th November, 1947. — W. D. Rannie

"Heat transfer in sweat-cooled porous metals". Journal of Applied Physics, Vol.20, January, 1949. — S. Weinbaum and H. L. Wheeler

"Some observations on the mechanism of sweat-cooling". Proc. VIIth International Congress for Applied Mechanics. London, September, 1948. — P. Grootenhuis and N. P. W. Moore

"On sweat-cooling". Journal of Aeronautical Sciences, Vol.16, No.1, January, 1949. — E. A. Richardson

"Porous cooling". Journal of Aeronautical Sciences, Vol.16, No.4, April, 1949. — L. Lees

"Stability of the boundary layers and of flow in entrance section of a channel". Journal of Aeronautical Sciences, Vol.15, No.8, August, 1948. — H. Hahnemann and J. C. Freeman

BIBLIOGRAPHY (Cont'd.)

| | Author(s) |
|---|---|
| "The stability of the laminar boundary layer with injection of a cool gas at the wall". Princeton University, Aeronautical Engineering Laboratory. Report No.139, 20th May 1948, P.16252. | L. Lees |
| "Heat transfer in laminar compressible boundary layer on a porous flat plate with fluid injection". Journal of the Aeronautical Sciences, Vol.16, No.12, December 1949. | S. W. Yuan |
| "Sweat-cooling". The Engineer, 24th February, 1950. p.230. | N. P. W. Moore and P. Grootenhuis |
| "Some factors in the use of high temperatures in gas turbines" presented at the Institute of Mechanical Engineers, 27th January 1950. | T. W. F. Brown |
| "Heat transfer characteristics of cooled gas turbine blades". General Discussion of Heat Transfer Section. V.- Special problems. London Conference at the Institute of Mechanical Engineers, 11-13th September 1951. | H. L. Ellerbrock |
| "Heat transfer and temperature profiles in laminar boundary layers on a sweat-cooled wall". Tech. Rept. No.5646 Air Materiel Command, 3rd November 1947. | E. Eckert |
| "A theoretical and experimental investigation of Rocket Motor sweat cooling". Journal Amer. Rocket Soc. No.79, December 1949, pp.147-154. | J. Friedman |
| "Exact solutions of the laminar boundary layer equations for a porous plate with variable fluid properties and a pressure gradient in the main stream". Paper presented before the first U.S. National Congress of Applied Mechanics, Chicago, Illinois, 11-16th June 1951. | B. Brown |

## APPENDIX I

### Symbols

| | | Dimensions |
|---|---|---|
| $c$ | Blade chord | ft. |
| $C$ | Injection parameter defined in Equation 9, Appendix II. | Dimensionless |
| $C_p$ | Specific heat at constant pressure | CHU lb.$^{-1}$ °C.$^{-1}$ |
| $f\left(\frac{T_b}{T_g}\right)$ | Heat transfer correction for temperature ratio in a laminar boundary layer defined in Equation 13, Appendix IV. | Dimensionless |
| $f_1\left(\frac{T_b}{T_g}\right)$ | Heat transfer correction for temperature ratio in a turbulent boundary layer defined in Equation 7, main text. | Dimensionless |
| $f(\eta)$ | Function of $\eta$ defined by Equation 7, Appendix II. | Dimensionless |
| $F(\eta)$ | Function of $\eta$ defined by Equation 3, Appendix IV. | Dimensionless |
| $J(\eta)$ | Function of $\eta$ defined by Equation 3, Appendix IV. | Dimensionless |
| $K$ | Constant in Equations 4 and 5, Appendix II. | Dimensionless |
| $m$ | Wedge parameter $= \frac{\beta}{2-\beta}$ | Dimensionless |
| $Nu$ | Nusselt number $\frac{\alpha \ell}{\lambda}$ | Dimensionless |
| $p$ | Dependent variable in Equation 2, Appendix III $= f'(\eta)$. | ft. sec.$^{-1}$ |
| $Pr$ | Prandtl number $\frac{\mu C_p}{\lambda}$ | Dimensionless |
| $q$ | Coolant mass flow per unit area per sec. $= V_\rho$ | lb. ft.$^{-2}$ sec.$^{-1}$ |
| $Q$ | Mainstream mass flow per unit area per sec. at blade exit $= U_o\rho$ $\left[\text{i.e. } U\rho \text{ at exit}\right]$ | lb. ft.$^{-2}$ sec.$^{-1}$ |
| $R$ | Blade nose radius | ft. |
| $Re$ | Reynolds number $\frac{Uc\rho}{\mu}$ | Dimensionless |
| $s$ | Distance from stagnation point to trailing edge measured along curved surface, or an arbitrary standard length in the case of a wedge. | ft. |
| $T$ | Temperature (absolute). | °K. |
| $u$ | Velocities parallel to surface in boundary layer. | ft. sec.$^{-1}$ |
| $U$ | Velocity parallel to surface at edge of boundary layer. | ft. sec.$^{-1}$ |

## APPENDIX I (Cont'd.)

### Symbols

| | | Dimensions |
|---|---|---|
| $v$ | Velocity normal to surface in boundary layer. | ft. sec.$^{-1}$ |
| $V$ | Velocity normal to surface at wall. | ft. sec.$^{-1}$ |
| $x$ | Distance measured along the surface | ft. |
| $y$ | Distance measured normal to the surface | ft. |
| $Zt^*$ | Dimensionless temperature boundary layer thickness defined by Equation 6, Appendix IV. | Dimensionless |
| $\alpha$ | Heat transfer coefficient | CHU ft.$^{-2}$ °C.$^{-1}$ sec.$^{-1}$ |
| $\beta$ | $\left[\dfrac{\text{Included wedge angle}}{\pi}\right]$ | Dimensionless |
| $\gamma$ | Constant in Equation 4, Appendix II | Dimensionless |
| $\delta t^*$ | Temperature boundary layer thickness | ft. |
| $\Delta_2$ | Dimensionless momentum thickness | Dimensionless |
| $\varepsilon$ | Constant in Equation 5, Appendix II | Dimensionless |
| $\lambda$ | Thermal conductivity | CHU ft.$^{-1}$ °C.$^{-1}$ sec.$^{-1}$ |
| $\lambda t^*$ | Form parameter defined by Equation 8, Appendix IV. | Dimensionless |
| $\rho$ | Density | lb. ft.$^{-3}$ |
| $\theta$ | Dimensionless temperature in boundary layer defined in Appendix III. | Dimensionless |
| $\mu$ | Viscosity | lb. ft.$^{-1}$ sec.$^{-1}$ |
| $\eta$ | Dimensionless distance perpendicular to surface defined by Equation 7, Appendix II. | Dimensionless |
| $\psi$ | Stream function, see Equation 7, Appendix II. | ft.$^2$ sec.$^{-1}$ |
| $\nu$ | Dynamic viscosity | ft.$^2$ sec.$^{-1}$ |

## SUFFICES

| | |
|---|---|
| g | Refers to gas or fluid |
| b | Refers to blade or body |
| c | Refers to coolant |
| o | Refers to blade exit |
| x | Refers to value at point x, e.g. $Nu_x = \frac{\alpha x}{\lambda}$ $Re_x = \frac{Ux\rho}{\mu}$ |
| s | Refers to value at point s, e.g. $Nu_s = \frac{\alpha s}{\lambda}$ $Re_s = \frac{U_o s\rho}{\mu}$ |
| 1 | Refers to the convex blade surface |
| 2 | Refers to the concave blade surface |

APPENDIX II

Solution of the dynamic boundary layer equations

The boundary layer equations for two dimensional incompressible, isothermal laminar flow are:

$$u\frac{\partial u}{\partial x} + v\frac{\partial u}{\partial y} = \nu\frac{\partial^2 u}{\partial y^2} + U\frac{dU}{dx} \qquad \ldots \quad (1)$$

$$\frac{\partial u}{\partial x} + \frac{\partial v}{\partial y} = 0 \qquad \ldots \quad (2)$$

with the boundary conditions

$$y = 0,\ u = 0,\ v = V$$

$$y \to \infty \quad u = U \qquad \ldots \quad (3)$$

It has been shown that in order that "similar" solutions of the above equations may be obtained, the velocity distribution over the surface considered must be of the form

$$U = K_1\left[(2\gamma - \beta)\frac{x}{s}\right]^{\frac{\beta}{2-\beta}} \qquad \ldots \quad (4)$$

or, in the special case where $2\gamma - \beta = 0$

$$U = K_2 e^{\frac{\beta}{\varepsilon}\frac{x}{s}} \quad \text{(Reference 4)} \qquad \ldots \quad (5)$$

If $\gamma = 1$ in Equation 4, we obtain the velocity distribution as over a semi-infinite wedge of included angle $\beta\pi$. Although solutions have been obtained for other values of $\gamma$, the only value of interest in this report is $\gamma = 1$, and $\beta$ ranging from 0.1988 to 1.0000.

Equation 4, re-written with $\gamma = 1$ gives us

$$U = K\left(\frac{x}{s}\right)^{\frac{\beta}{2-\beta}} \qquad \ldots \quad (6)$$

Equations 1, 2, may be readily converted into a non-linear total differential equation by changing the variables from u, v, x, y, to $\eta$ and $f(\eta)$, the latter functions being defined by:

$$\eta = \frac{1}{\sqrt{2-\beta}}\sqrt{\frac{U}{\nu x}}\,y$$

$$\psi = \sqrt{2-\beta}\,\sqrt{U\nu x}\,f(\eta) \qquad \ldots \quad (7)$$

$$\left(\text{Note:}\quad u = \frac{\partial\psi}{\partial y}\quad v = -\frac{\partial\psi}{\partial x}\right)$$

APPENDIX II (Cont'd.)

Hence $\frac{u}{U} = f' (\eta)$

and

$$V = \frac{-1}{\sqrt{2 - \beta}} \sqrt{\frac{U\nu}{x}} \left\{ f \;(\eta) + (\beta - 1)\; \eta f' \;(\eta)\right\}$$

and equations 1, 2, resolve to

$$f''' (\eta) + f (\eta)\, f'' (\eta) = \beta \left\{ f' (\eta)^2 - 1 \right\} \quad .. \quad .. \quad .. \qquad (8)$$

with boundary conditions

$$\eta = 0,\; f' (\eta) = 0,\; f (\eta) = - \sqrt{2 - \beta}\; \frac{V}{U} \sqrt{\frac{Ux}{\nu}} = C \quad .. \quad .. \quad .. \qquad (9)$$

$$\eta \to \infty \;\; f' (\eta) = 1$$

This Equation may be solved by a relaxation process (see Appendix III).

## APPENDIX III

### Note on the method of computing similar solutions of the boundary layer equations

It has been previously shown that the isothermal dynamic boundary layer equations may be transformed to the non-linear total differential equation (see Appendix II).

$$f'''(\eta) + f(\eta)\, f''(\eta) = \beta \left\{ f'(\eta)^2 - 1 \right\} \quad \ldots \quad \ldots \quad \ldots \quad (1)$$

As equations of odd orders are difficult to solve by relaxation processes, equation (1) is integrated to give the second order equation

$$p'' + p' \left[ f(o) + \int_0^{\eta} p\,d\eta \right] - \beta \left\{ p^2 - 1 \right\} = 0 \quad \ldots \quad \ldots \quad \ldots \quad (2)$$

where $f'(\eta)$, the dependent variable, is replaced by p.

The quantity is squared brackets (Equation 2) at any point $\eta$ is replaced by the symbol $g_\eta$ to simplify later formulae.

We can replace Equation 2, by a finite difference equation[16] the equation becoming

$$p_{\eta+h}(1 + \tfrac{1}{2} hg_\eta) + p_{\eta-h}(1 - \tfrac{1}{2} hg_\eta) - 2p_\eta - \beta h^2 (p_\eta^2 - 1) + \Delta = 0 \quad \ldots (3)$$

where $\Delta$, the difference correction $= -\dfrac{hg}{6}\delta^3{}_0 - \dfrac{1}{12}\delta^4{}_0 + \dfrac{hg}{30}\delta^5{}_0 + \dfrac{1}{90}\delta^6{}_0 \ldots$ (4)

and the interval is h.

Equation (3) is solved by successive approximations; the left hand side being called the residual R, and the relaxation process being to reduce this residual to zero. The relaxation equation or the equation connecting the change in residual with the change in p is obtained from this equation neglecting the effect of a change in p on the difference corrections.

Thus the two relevant equations are:-

$$p_{\eta+h}(1 + \tfrac{1}{2} hg_\eta) + p_{\eta-h}(1 - \tfrac{1}{2} hg_\eta) - 2\, p_\eta - \beta h^2 (p_\eta^2 - 1) + \Delta = R \quad \ldots (5)$$

$$\Delta p_{\eta+h}(1 + \tfrac{1}{2} hg_\eta) + \Delta p_{\eta-h}(1 - \tfrac{1}{2} hg_\eta) - 2\Delta p_\eta - 2\beta h^2\, p_\eta \Delta p_\eta = \Delta R \quad \ldots (6)$$

The integral $\int_0^{\eta} p\,d\eta$ is evaluated in the later stages of the relaxation process using central difference integration formula.

APPENDIX III (Cont'd.)

$$\int_0^{\eta} p d_{\eta} = h \left\{ 'f_o - \frac{1}{12}\delta'_o + \frac{11}{720}\delta^3_o - \frac{191}{60,480}\delta^5_o + \frac{2,497}{3,628,800}\delta^7_o \right\} \qquad (7)$$

$'f_o$, the first sum is adjusted so that the integral at $\eta = 0$ is zero, i.e.

$$'f_o = \frac{1}{12}\delta'_o - \frac{11}{720}\delta^3_o \ldots\ldots \qquad (8)$$

$g_{\eta}$ can easily be evaluated knowing the above integral, as the value of $f(0) = C$ is known.

Details of method of solution

1. Values of p were guessed at intervals h. The interval h was chosen as either 0.5 or 1.0, the larger intervals being chosen when the value of $\eta$ at which p approached unity was expected to be large.

If other solutions are available with values of $\beta$ and f(0) near to that required, a close approximation to the values of p may be obtained by interpolation or extrapolation.

2. The integral $\int_0^{\eta} p d_{\eta}$ in the first instance was obtained using Simpson's rule. The difference method of integration could not be used at this stage because the difference table was unreliable.

3. The residuals (i.e. the left hand side of Equation 4) were calculated at each point, the difference correction being neglected at this stage. One more figure was kept in the residuals than in the values of p.

4. The residuals calculated in 3 were relaxed using Equation 6 to almost zero neglecting the dependence of the function $g_{\eta}$ on p.

5. Steps 2, 3 and 4 were repeated until the successive values of p, correct to two decimal places, were very nearly equal.

6. A difference table was made of the function p up to the order at which the differences ceased to vary smoothly. It is necessary to estimate the differences at the beginning of the table by extrapolation. The process adopted was to plot a graph of the first order differences against $\eta$ and assume the difference zero at $\eta = 0.25$.

Any central differences required were obtained from the arithmetical mean of the adjacent forward and backward differences.

7. The integral $\int_0^{\eta} p d_{\eta}$ was integrated using the central difference formula (Equations 7, 8). One more figure was kept in the integral than in p.

8. The residuals were again calculated (Equations 3, 4) incorporating as many terms of the difference correction as necessary.

APPENDIX III (Cont'd.)

9. The residuals again relaxed to nearly zero as in 5

10. Steps 6, 7, 8 and 9 were repeated, increasing the number of decimal places as the accuracy of the solution increases.

Comments on solutions obtained

For small and negative values of $\beta$ the process took longer as large changes in p were necessary to relax a small residual. Also the residuals had to be calculated to more decimal places than would be needed if $\beta$ were large. With negative values of $\beta$ the usual solutions could be obtained up to a critical value of $f(0)$ but the reversed flow solution could not be obtained unless the initial estimate of p was made with very high accuracy.

When $\beta = 0$, the boundary layer thickness increased very rapidly as $f(0)$ approached -0.8. No solutions were obtained for $f(0) < -0.8$ because of the extremely large values of $\eta$ at which $p \to 1$.

# APPENDIX IV

## Solution of the thermal boundary layer equation

When solving the differential equation controlling the temperature field for high speed flow it is usual to neglect those terms concerning dissipation, dissipation being allowed for by considering the effective temperature of the moving gas to be the static temperature plus 0.86 of its kinetic temperature at the edge of the boundary layer.

Thus the equation we have to solve is:

$$u \frac{\partial T}{\partial x} + v \frac{\partial T}{\partial y} = \frac{\lambda}{\rho C_p} \frac{\partial^2 T}{\partial y^2} \quad \ldots \ldots \ldots \ldots \ldots \quad (1)$$

with the boundary conditions

$$y = 0, \; t = T_b$$

$$y \to \infty \quad t = T_g$$

Substituting the variables $\eta$ and $f(\eta)$ from Appendix II and replacing T by $\theta$, $\theta$ being defined as $\frac{T - T_b}{T_g - T_b}$, we transform Equation (1) into a simple second degree, first order equation which can be readily solved by separating the variables and integrating.

Equation (1) becomes

$$\frac{d^2\theta}{d\eta^2} + Pr\, f(\eta) \frac{d\theta}{d\eta} = 0 \quad \ldots \ldots \ldots \ldots \ldots \ldots \ldots \quad (2)$$

with the boundary conditions

$$\eta = 0, \; \theta = 0$$

$$\eta \to \infty \quad \theta = 1$$

And the solution for $\theta$ is

$$\theta = \frac{J(\eta)}{J(\infty)}; \; J(\eta) = \int_0^{\eta} e^{-F(\eta)}\, d\eta \; ; \; F(\eta) = Pr \int_0^{\eta} f(\eta)\, d\eta \quad \ldots \ldots \ldots \quad (3)$$

APPENDIX IV (Cont'd.)

We can also find that $\frac{Nu_x}{\sqrt{Re_x}} = \frac{1}{\sqrt{2 - \beta}} \frac{1}{J(\infty)}$ .. .. .. .. (4)

It is important to note that the above solution implies that $T_b$ and $T_g$ are constant. If one or both of these temperatures vary, important changes in the temperature profile and heat transfer may occur.

We define the displacement thickness of the temperature boundary layers as:

$$\delta t^* = \int_0^\infty (1 - \theta)\, dy$$

$$= \sqrt{2 - \beta} \sqrt{\frac{\nu x}{U}} \int_0^\infty (1 - \theta)\, d\eta \quad .. \quad .. \qquad (5)$$

or, on writing $Zt^*$ for $\int_0^\infty (1 - \theta)\, d\eta$

$$\delta t^* = \sqrt{2 - \beta} \sqrt{\frac{\nu x}{U}}\, Zt^*$$

where $Zt^*$ is a function of C, $\beta$ and Pr .. .. .. .. .. (6)

As the origin of the boundary layer is indeterminate, it is desirable to eliminate x from the above expression. Because the flow is that over a semi-infinite wedge we have

$$\frac{U}{U_o} = K \left(\frac{x}{s}\right)^{\frac{\beta}{2 - \beta}}$$

Differentiating we obtain $\frac{x}{s} = \frac{\beta}{2 - \beta} \frac{U/U_o}{\frac{d\,(U/U_o)}{d\,(x/s)}}$ .. .. .. .. (7)

Squaring Equation (6) and eliminating x using (7)

$$\beta\, Zt^{*2} = \left\{ \frac{\delta t^*}{s} \sqrt{Re_s} \right\}^2 \frac{d\,(U/U_o)}{d\,(x/s)} = \lambda t^* \quad .. \quad .. \qquad (8)$$

where $\lambda t^*$ is a function of C, $\beta$ and Pr only.

APPENDIX IV (Cont'd.)

Differentiating (6) with respect to x, $Zt^*$ and $\beta$ being constant we obtain

$$\frac{d\,\delta t^*}{dx} = \frac{1-\beta}{2-\beta}\,\frac{\delta t^*}{x}$$

Substituting for $\delta t^*$ from (6) the above equation becomes

$$\frac{d\,(\delta t^*/_s)\,\sqrt{Re_s}}{d\,(^x/_s)} = \frac{(1-\beta)\,Zt^{*2}}{U/U_o\;\delta t^*/_s\,\sqrt{Re_s}} \qquad \cdots\ \cdots\ \cdots \qquad (9)$$

In order that we may solve the boundary layer equations we still require a connection between C and $Zt^*$ or $\beta$. The expression for a constant surface temperature is obtained as follows:-

The heat balance equation for the surface cooling is

$$V\rho\,Cp\,(T_b - T_c) = \alpha\,(T_g - T_b)$$

Substituting for $\alpha$ from (4) we obtain the relationship

$$\frac{Nu_x}{\sqrt{Re_x}}\sqrt{2-\beta} = \frac{1}{J(\infty)} = -\,\frac{T_b - T_c}{T_g - T_b}\,Pr\,C \qquad \cdots\ \cdots\ \cdots \qquad (10)$$

Note that the left hand side is a function of C, $\beta$ and Pr.

The connection between C, $Zt^*$, $\delta t^*$ and the function $\frac{q}{Q}\sqrt{Re}$ for isothermal flow is obtained by eliminating x between the two equations.

$$C = -\,\frac{V}{U}\sqrt{\frac{Ux}{\nu}}\,\sqrt{2-\beta}$$

and

$$\delta t^* = \sqrt{2-\beta}\,\sqrt{\frac{\nu x}{U}}\,Zt^*$$

giving

$$\frac{V}{U_o}\sqrt{\frac{U_o s}{\nu}} = -\,\frac{C\,Zt^*}{\delta t^*/_s\,\sqrt{Re_s}} \qquad \cdots\ \cdots\ \cdots \qquad (11)$$

APPENDIX IV (Cont'd.)

By a similar means we can show that:-

$$\frac{Nu_s}{\sqrt{Re_s}} = \frac{Zt^*}{\delta t^*/_s \sqrt{Re_s}} \; \frac{1}{J(\infty)}$$

$$= \frac{T_b - T_c}{T_g - T_b} \, Pr \; \frac{V}{U} \sqrt{Re_s} \qquad \ldots \quad \ldots \quad \ldots \qquad (12)$$

If the flow is non-isothermal, modifications to the above equations are necessary.

The heat balance equation becomes:

$$V_{\rho b} \, C_{pb,c} \, (T_b - T_c) = \alpha \, (T_g - T_b)$$

Assuming that both the heat transfer coefficient and cooling air mass flow are reduced in the same proportion by the temperature ratio, this equation may be resolved into a similar form to equation 10, i.e.

$$\frac{Nu_x}{\sqrt{Re_x}} \sqrt{2 - \beta} = \frac{1}{J(\infty)} = -\left\{ \frac{(T_b - T_c)}{(T_g - T_b)} \; \frac{C_{pb,c}}{C_{pg}} \, Pr \right\} C \qquad \ldots \quad \ldots \quad \ldots \qquad (10a)$$

The values of $\frac{Nu}{\sqrt{Re}}$ and $\frac{q}{Q}\sqrt{Re}$ may be obtained by multiplying the isothermal value given by Equations (11) and (12) by a function of $\frac{T_b}{T_g}$, tentatively given by the equation:

$$f\left(\frac{T_b}{T_g}\right) = 0.7 + 0.3 \left(\frac{T_b}{T_g}\right) \qquad \ldots \quad \ldots \quad \ldots \quad \ldots \quad \ldots \quad \ldots \qquad (13)$$

i.e. $$\frac{q}{Q} \sqrt{Re_s} = - f\left(\frac{T_b}{T_g}\right) \frac{C \, Zt^*}{\delta t^*/_s \; \sqrt{Re_s}} \qquad \ldots \quad \ldots \quad \ldots \quad \ldots \quad \ldots \qquad (11a)$$

$$\frac{Nu}{\sqrt{Re}} = f\left(\frac{T_b}{T_g}\right) \frac{Zt^*}{\delta t^*/_s \sqrt{Re_s}} \; \frac{1}{J(\infty)} = \left\{ \frac{(T_b - T_c)}{(T_g - T_b)} \; \frac{C_{pb,c}}{C_{pg}} \, Pr \right\} \frac{q}{Q} \sqrt{Re_s} \qquad \ldots \qquad (12a)$$

## APPENDIX V

### Note on porosity, permeability and pressure drop in sintered materials

A porous material has two characteristics, the porosity and the permeability, the former being the ratio

$$\frac{\text{Specific gravity of metal - apparent specific gravity}}{\text{Specific gravity of metal}} \quad .. \quad (1)$$

and the latter being defined by

$$\text{Mass flow/unit area} = \text{permeability} \frac{\rho}{\mu} \frac{dp}{dl} \quad .. \quad .. \quad .. \quad (2)$$

and permeability has the units ft.$^2$. The permeability is constant only if the flow is laminar in the pores. As the temperature variation through the blade thickness is small the flow through the metal may be assumed to be isothermal. Hence pressure drop

$$= \frac{\text{Mass flow/unit area} \times 1 \times \mu \text{ mean}}{\text{permeability} \times \rho \text{ mean}} \quad .. \quad .. \quad .. \quad (3)$$

FIG. 1.

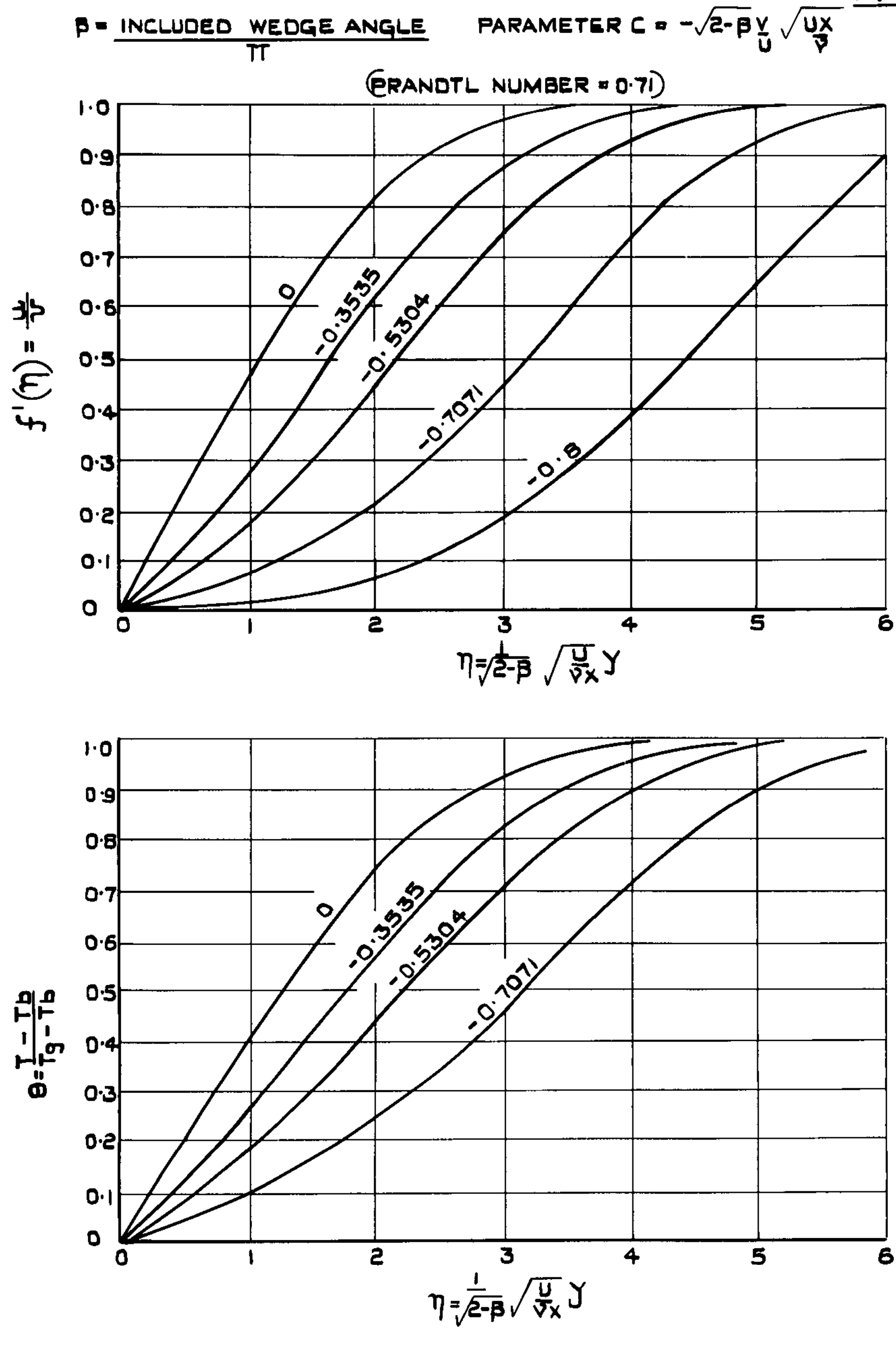


SOLUTIONS OF ISOTHERMAL BOUNDARY LAYER WITH GAS INJECTION

β = 0 (FLAT PLATE)

FIG. 2

$\beta = \dfrac{\text{INCLUDED WEDGE ANGLE}}{\pi}$ PARAMETER $C = -\sqrt{2-\beta}\,\dfrac{V}{U}\sqrt{\dfrac{Ux}{\nu}}$

(PRANDTL NUMBER = 0·71)

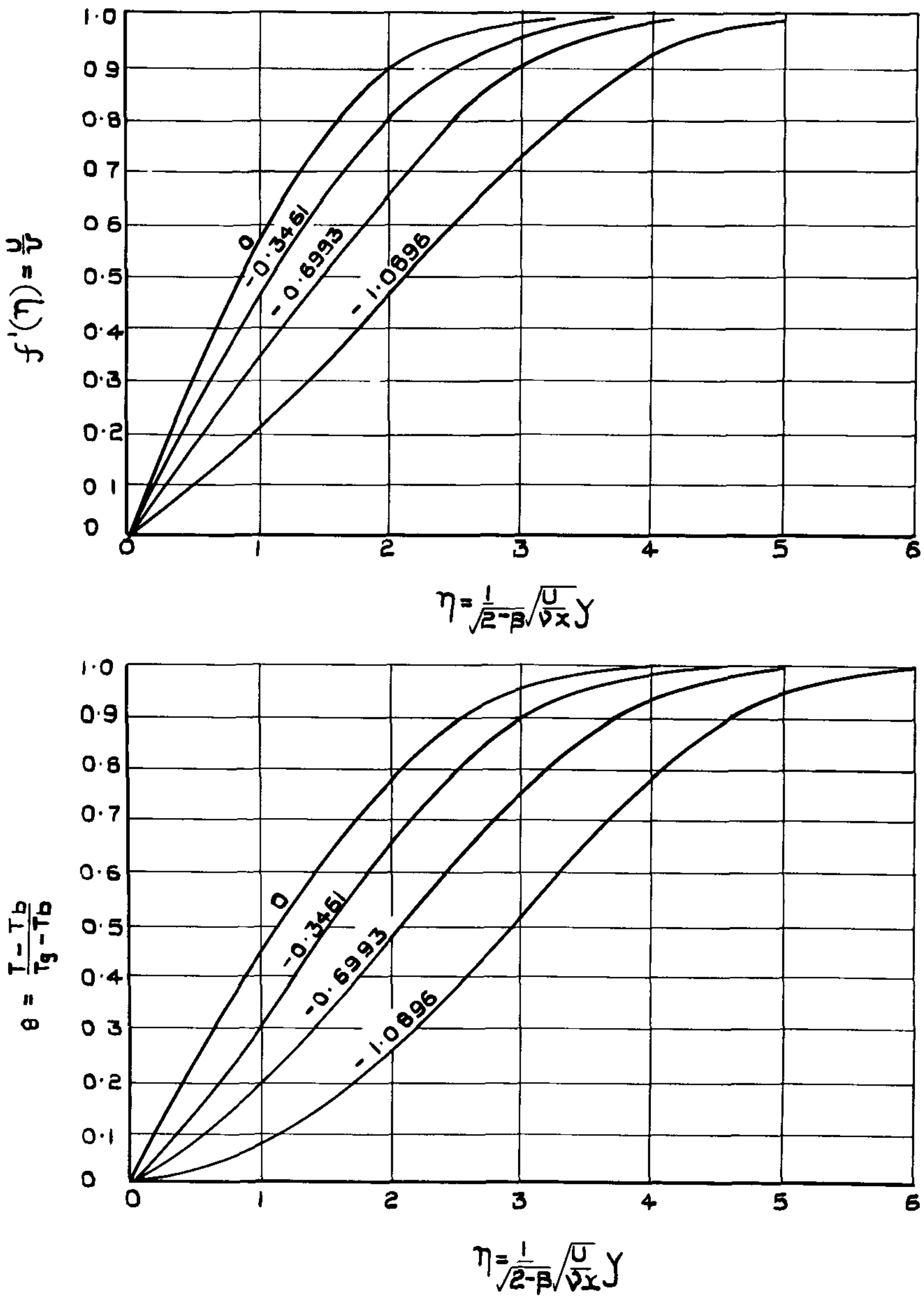


SOLUTIONS OF ISOTHERMAL BOUNDARY LAYER GAS INJECTION $\beta = 0{\cdot}2$.

FIG.3

$\beta = \frac{\text{INCLUDED WEDGE ANGLE}}{\pi}$ PARAMETER $C = -\sqrt{2-\beta}\ \frac{V}{U}\sqrt{\frac{UX}{\nu}}$

(PRANDTL NUMBER = 0·71)

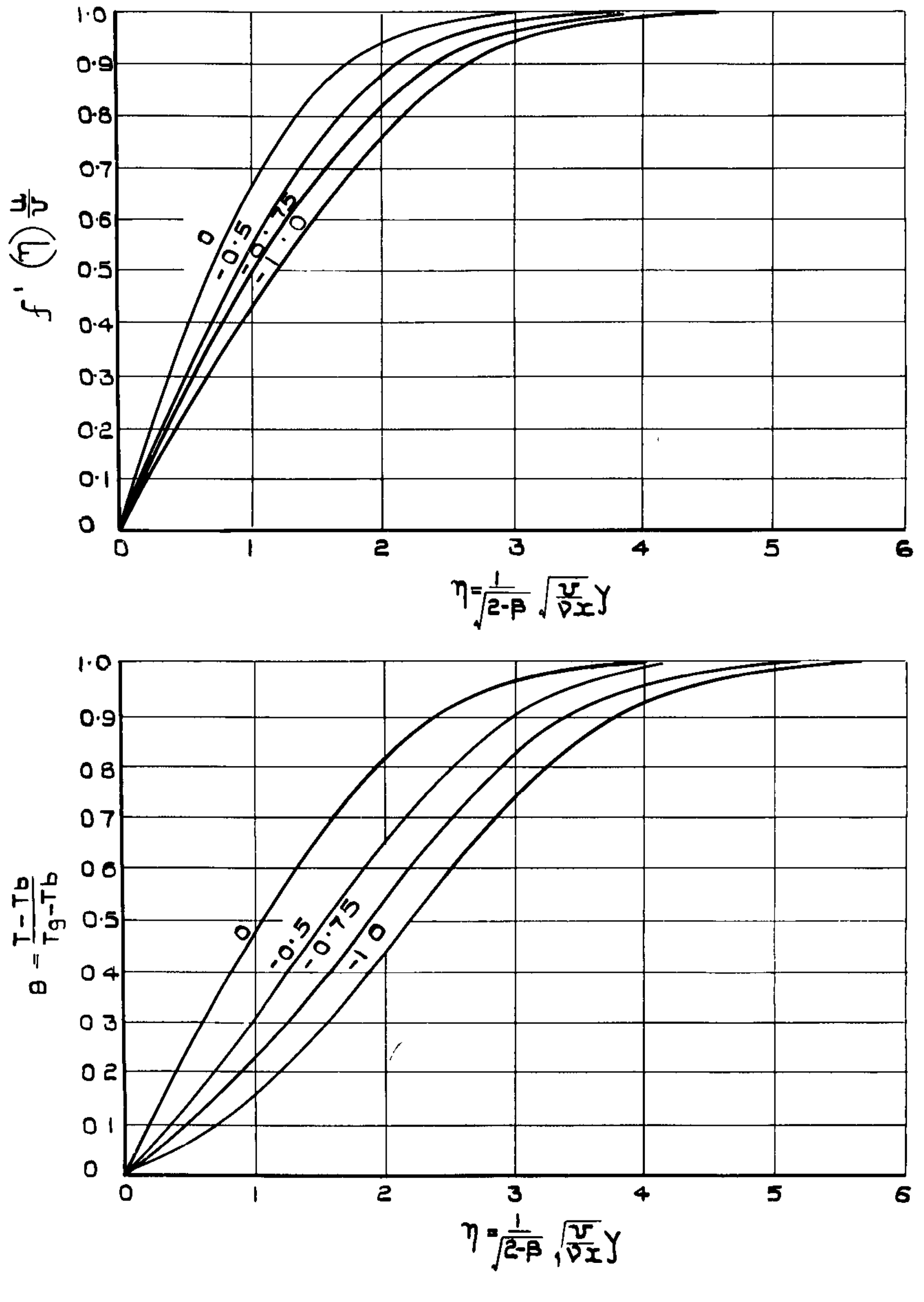


SOLUTIONS OF ISOTHERMAL BOUNDARY LAYER WITH GAS INJECTION $\beta = 0{\cdot}5$.

FIG. 4.

$\beta = \dfrac{\text{INCLUDED WEDGE ANGLE}}{\pi}$ PARAMETER $C = -\sqrt{2-\beta}\ \dfrac{V}{U}\sqrt{\dfrac{Ux}{\nu}}$

(PRANDTL NUMBER = 0·71)

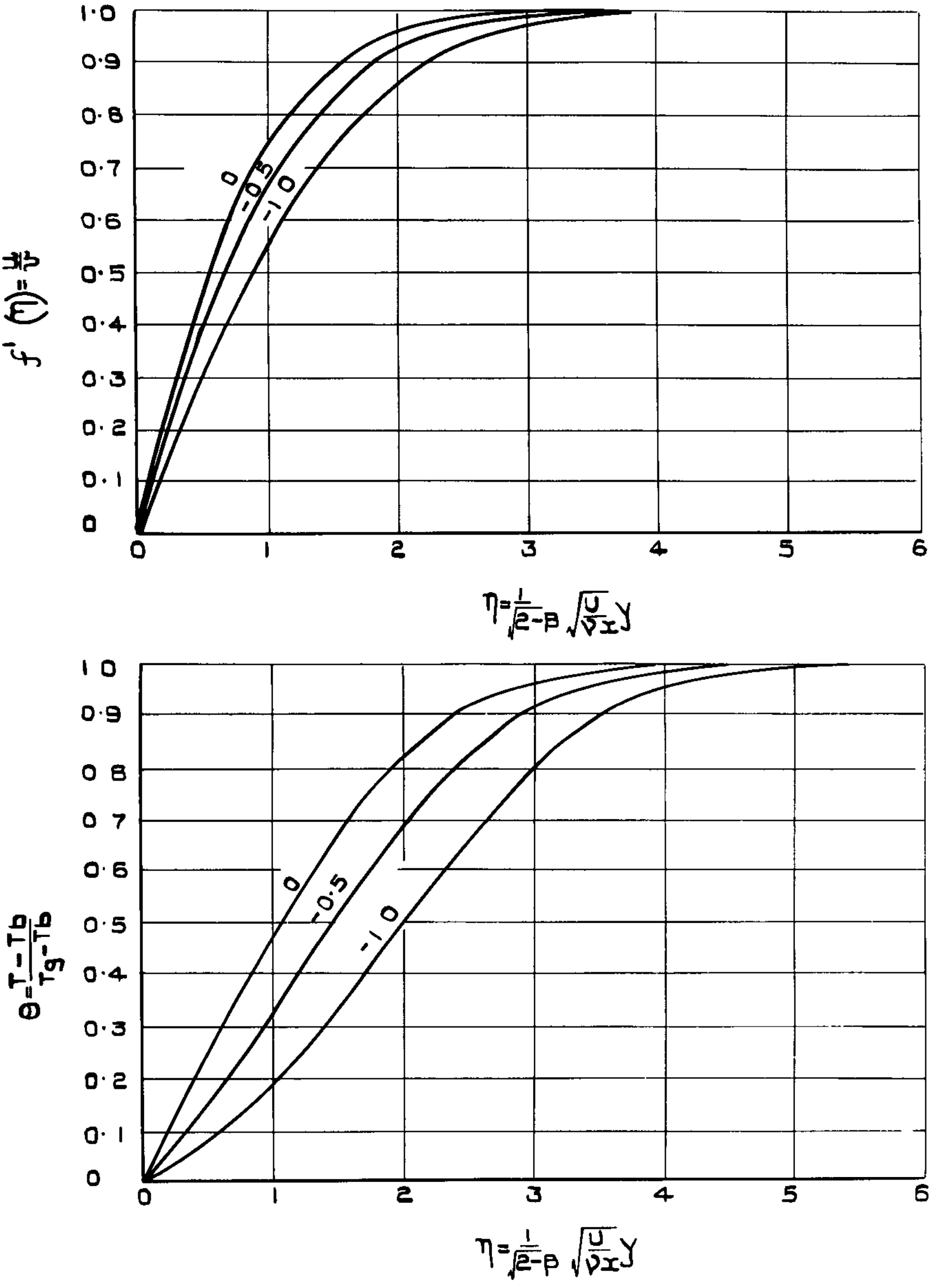


SOLUTIONS OF ISOTHERMAL BOUNDARY LAYER WITH GAS INJECTION $\beta = 0 \cdot 8$

FIG. 5.

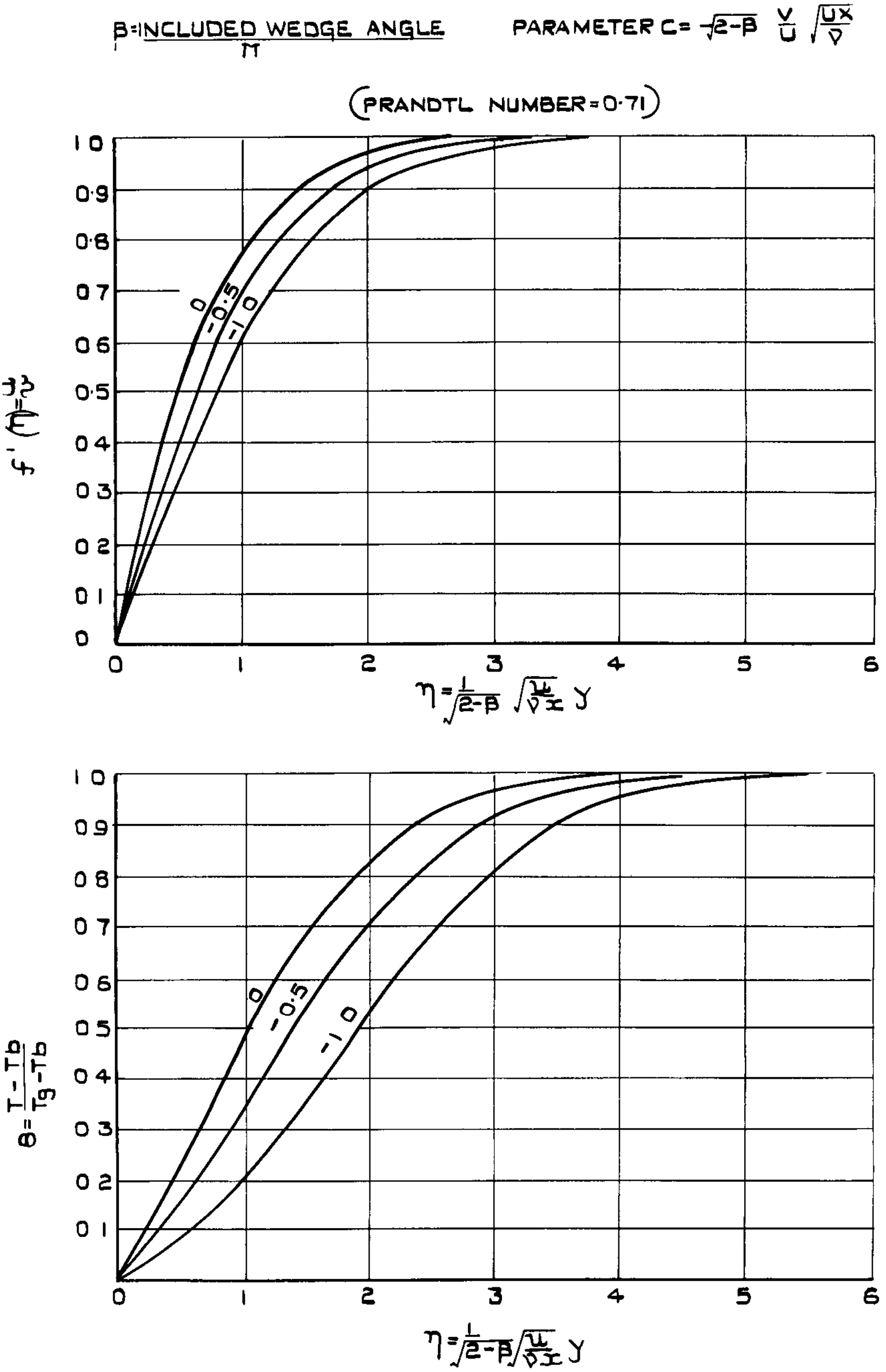


SOLUTIONS OF ISOTHERMAL BOUNDARY LAYER WITH GAS INJECTION β=1 (STAGNATION POINT)

FIG. 6.

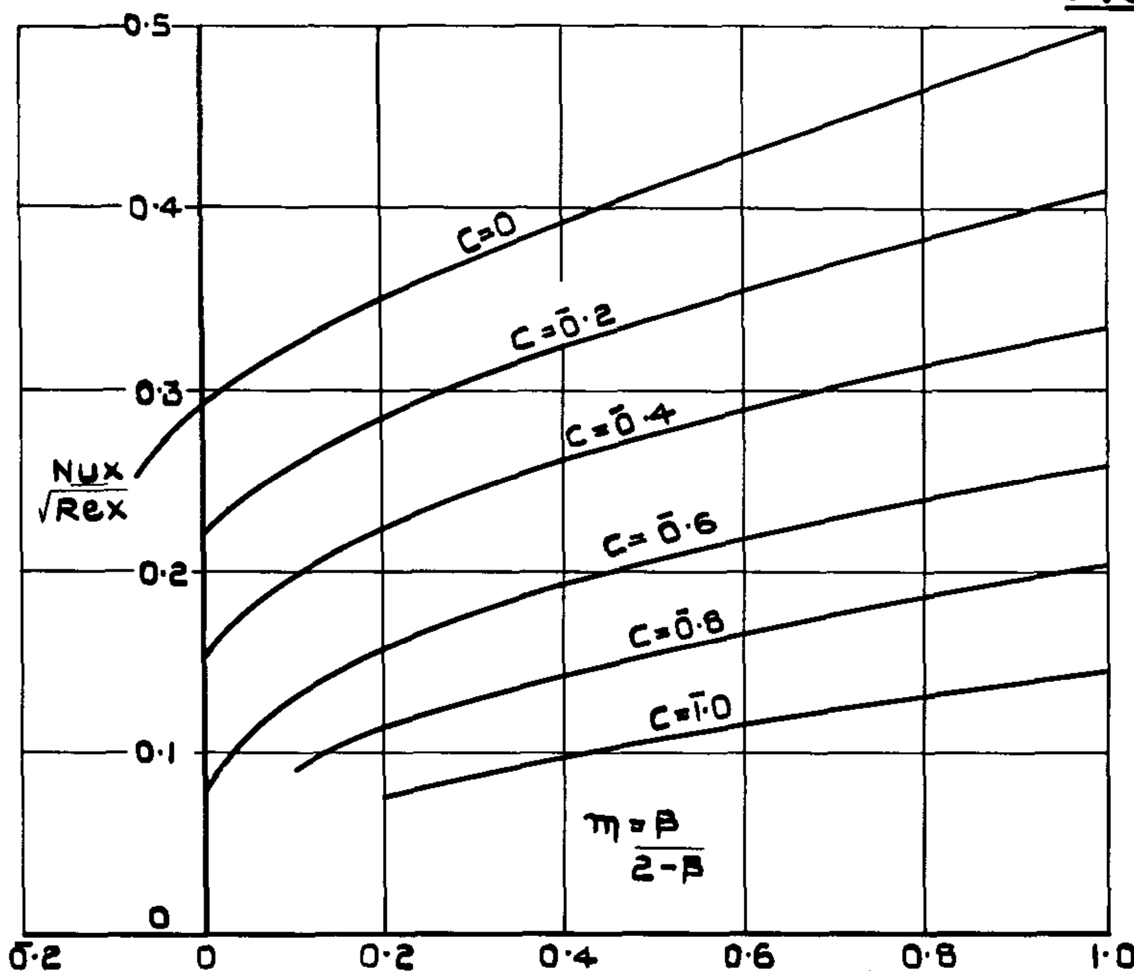


(a) DEPENDENCE OF THE RATIO $\frac{Nux}{\sqrt{Rex}}$ UPON INJECTION & PRESSURE DISTRIBUTION

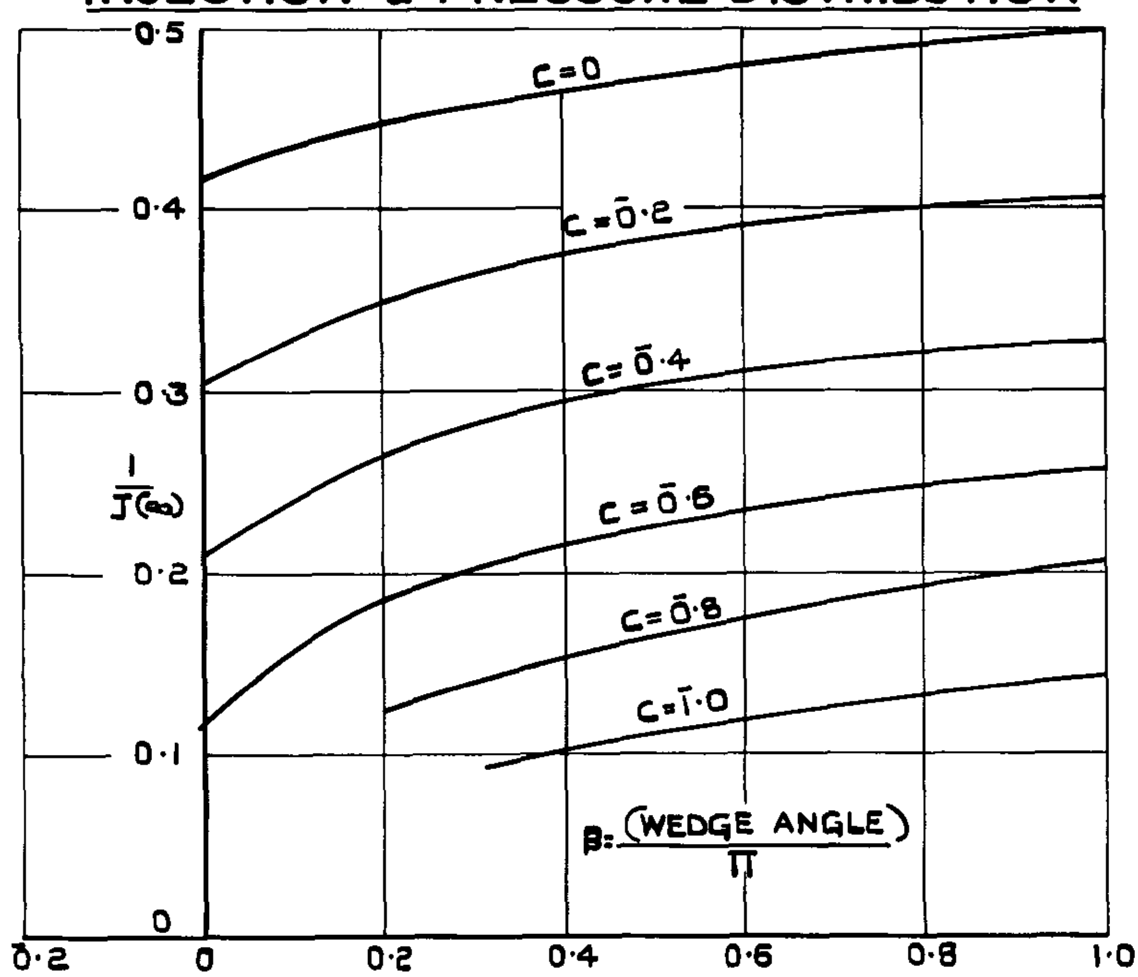


DEPENDENCE OF THE FUNCTION $\frac{1}{J(\infty)}$ UPON INJECTION & PRESSURE DISTRIBUTION.

FIG 7.

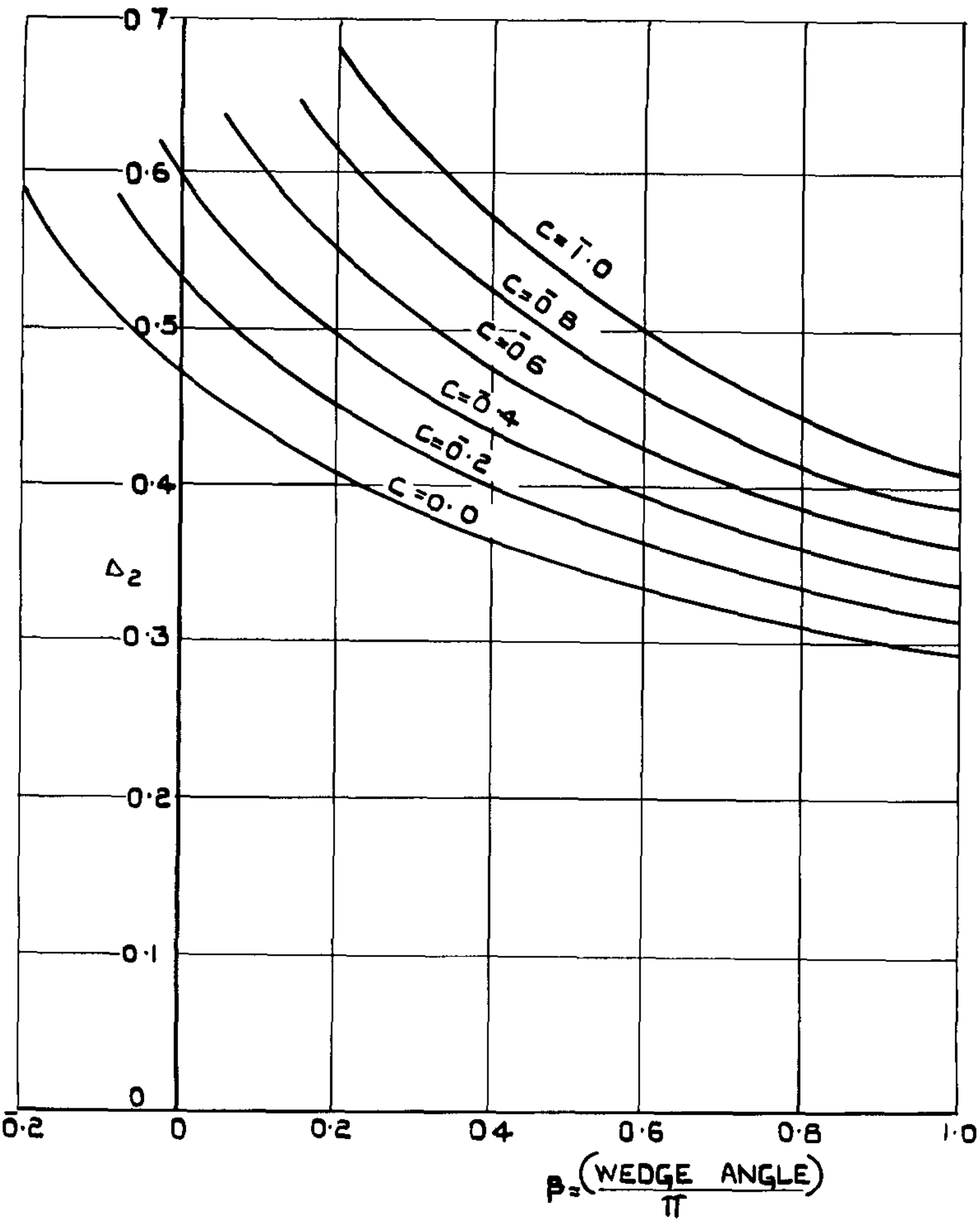


DEPENDENCE OF THE MOMENTUM THICKNESS $\Delta_2$ UPON THE PRESSURE DISTRIBUTION & AMOUNT OF INJECTION

FIG. 8.

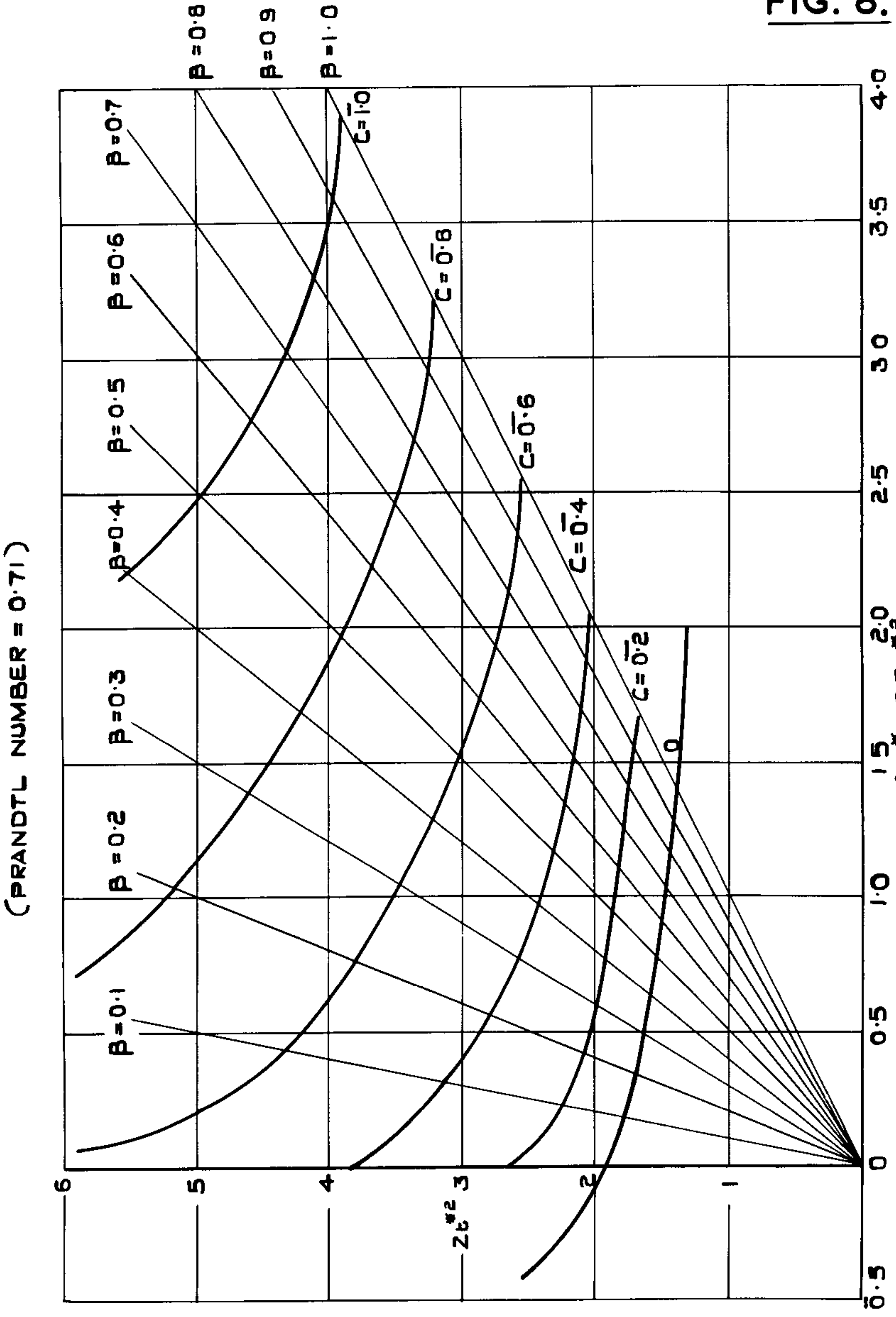


GRAPH FOR THE EVALUATION OF THE QUANTITY $Z_t^{*2}$ FROM THE FOR PARAMETER $\lambda_t^*$ AND THE INJECTION PARAMETER C

# FIG. 9.

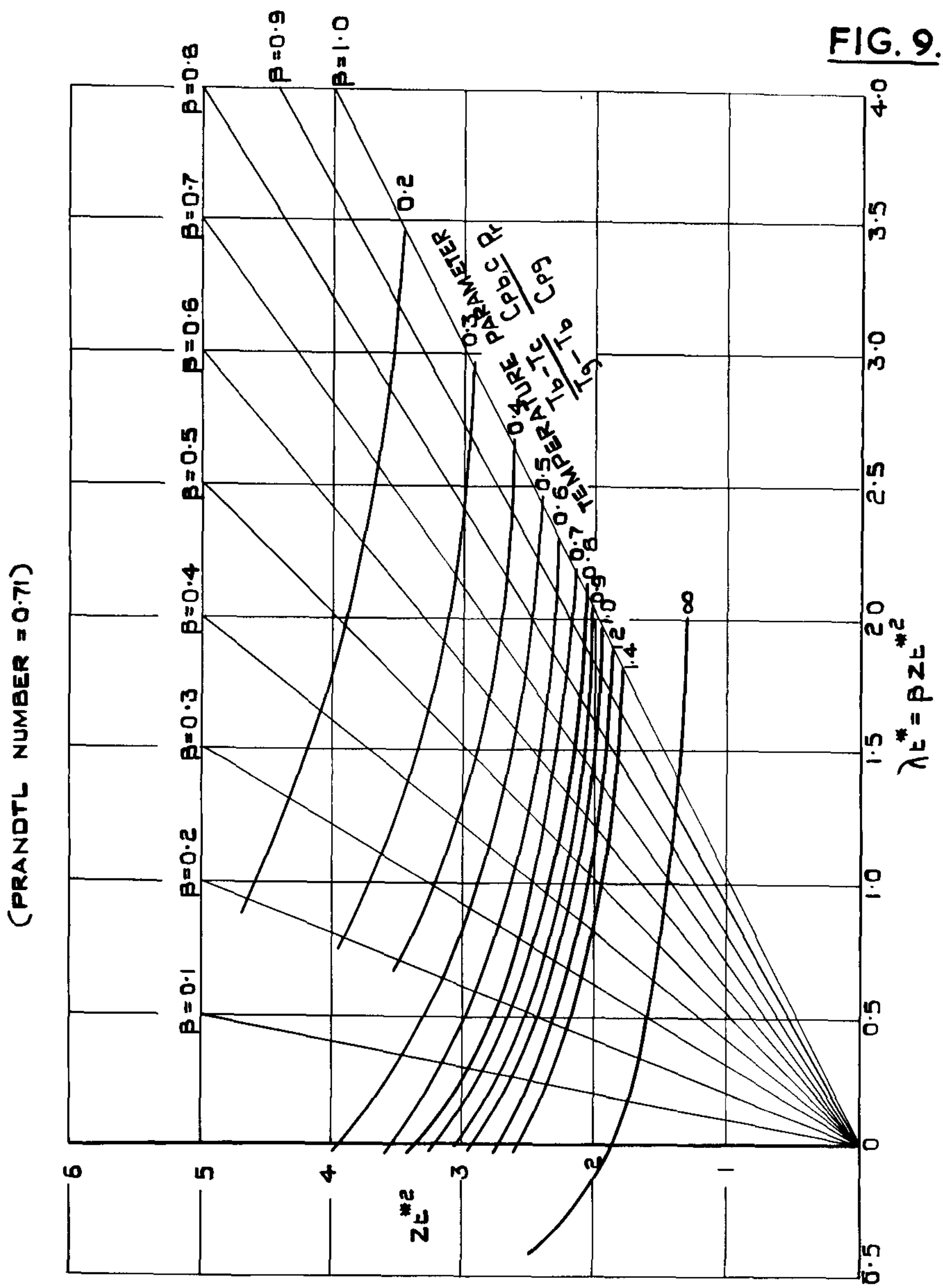


GRAPH FOR EVALUATION OF THE QUANTITY $Z_t^{*2}$ FROM THE FORM PARAMETER $\lambda_t^*$ AND THE TEMPERATURE PARAMETER.

FIG. 10.

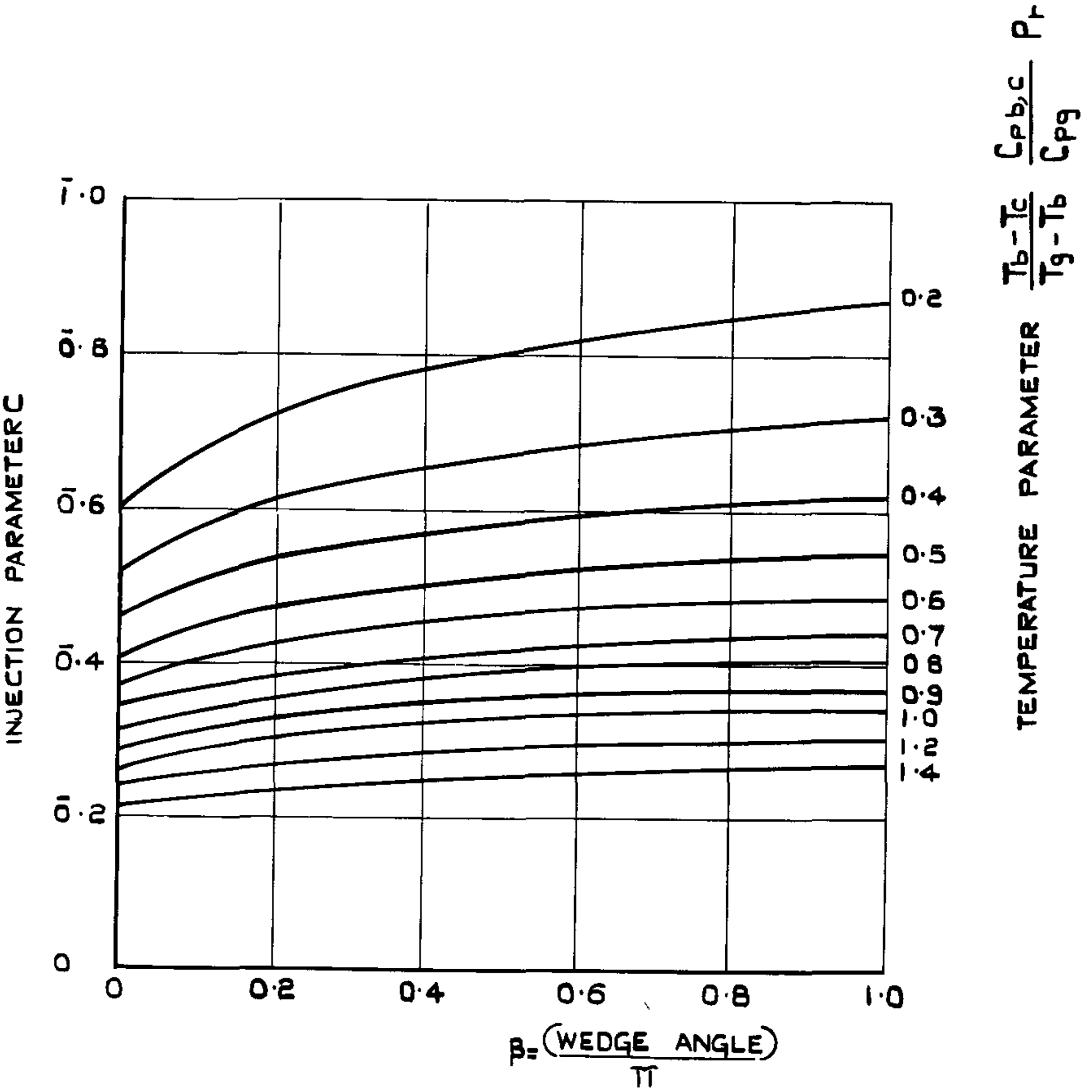


GRAPH FOR THE EVALUATION OF THE INJECTION PARAMETER C FOR A GIVEN WEDGE ANGLE (β) AND TEMPERATURE PARAMETER

FIG. 11.

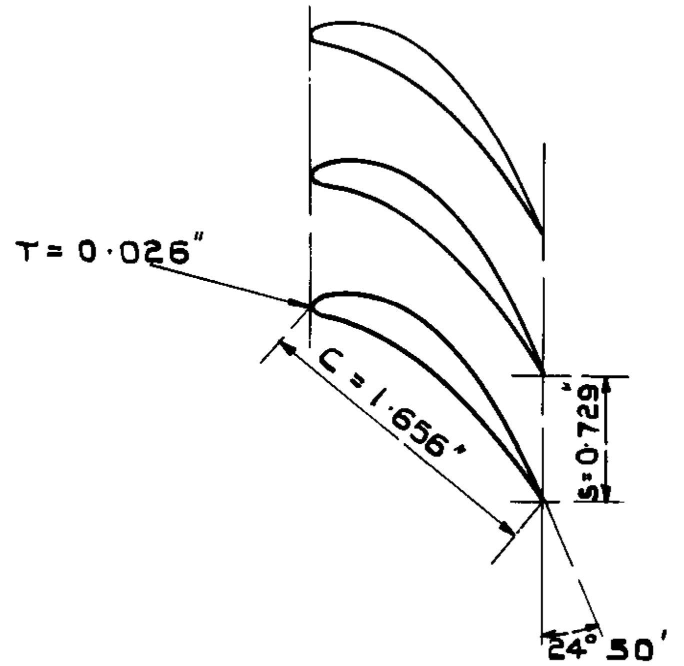


(a) DETAILS OF W2/700 NOZZLE GUIDE VANE CASCADE.

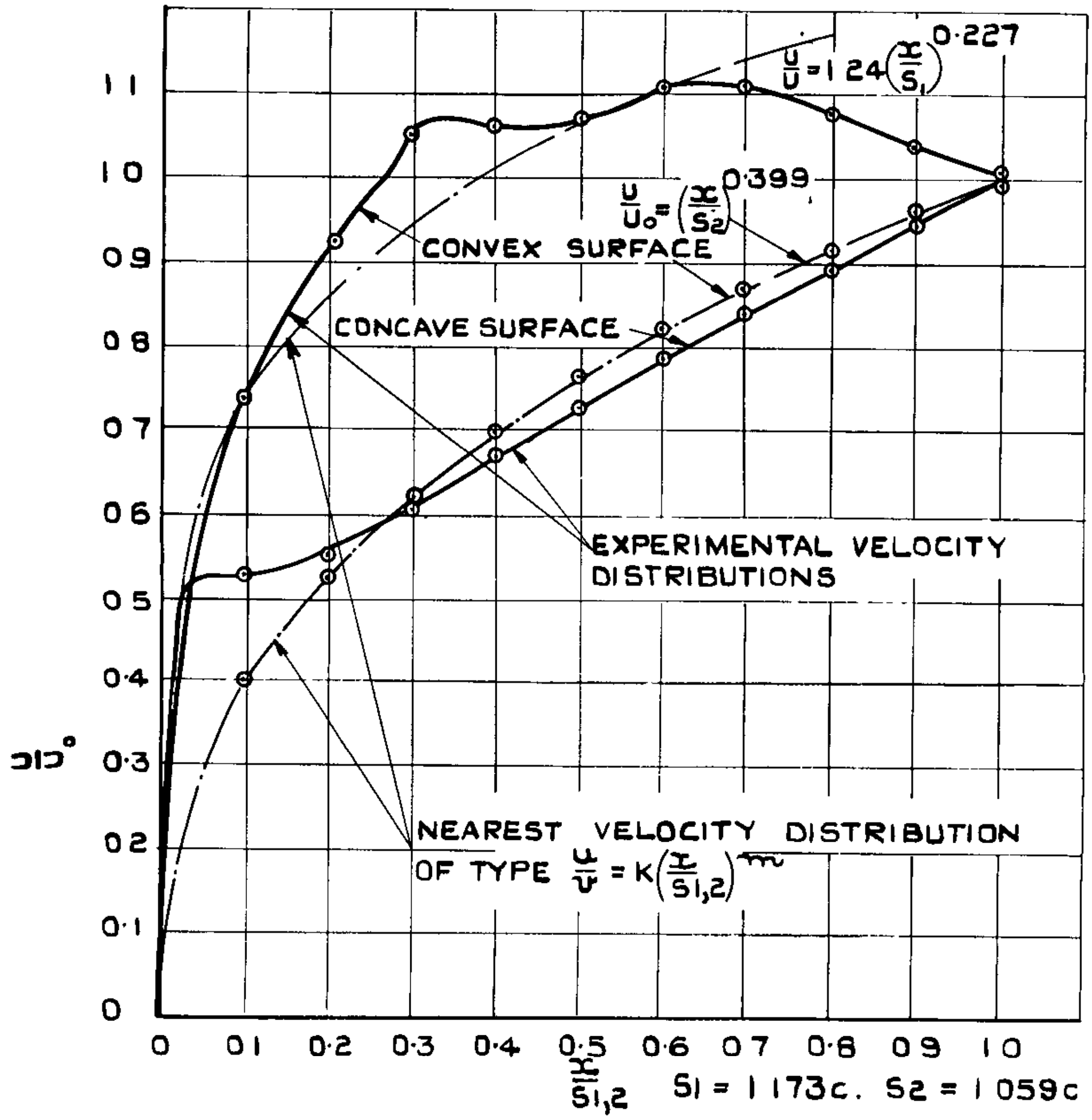


(b) VELOCITY DISTRIBUTION OVER THE SURFACE OF THE W2/700 NOZZLE GUIDE VANE.

FIG. 12.

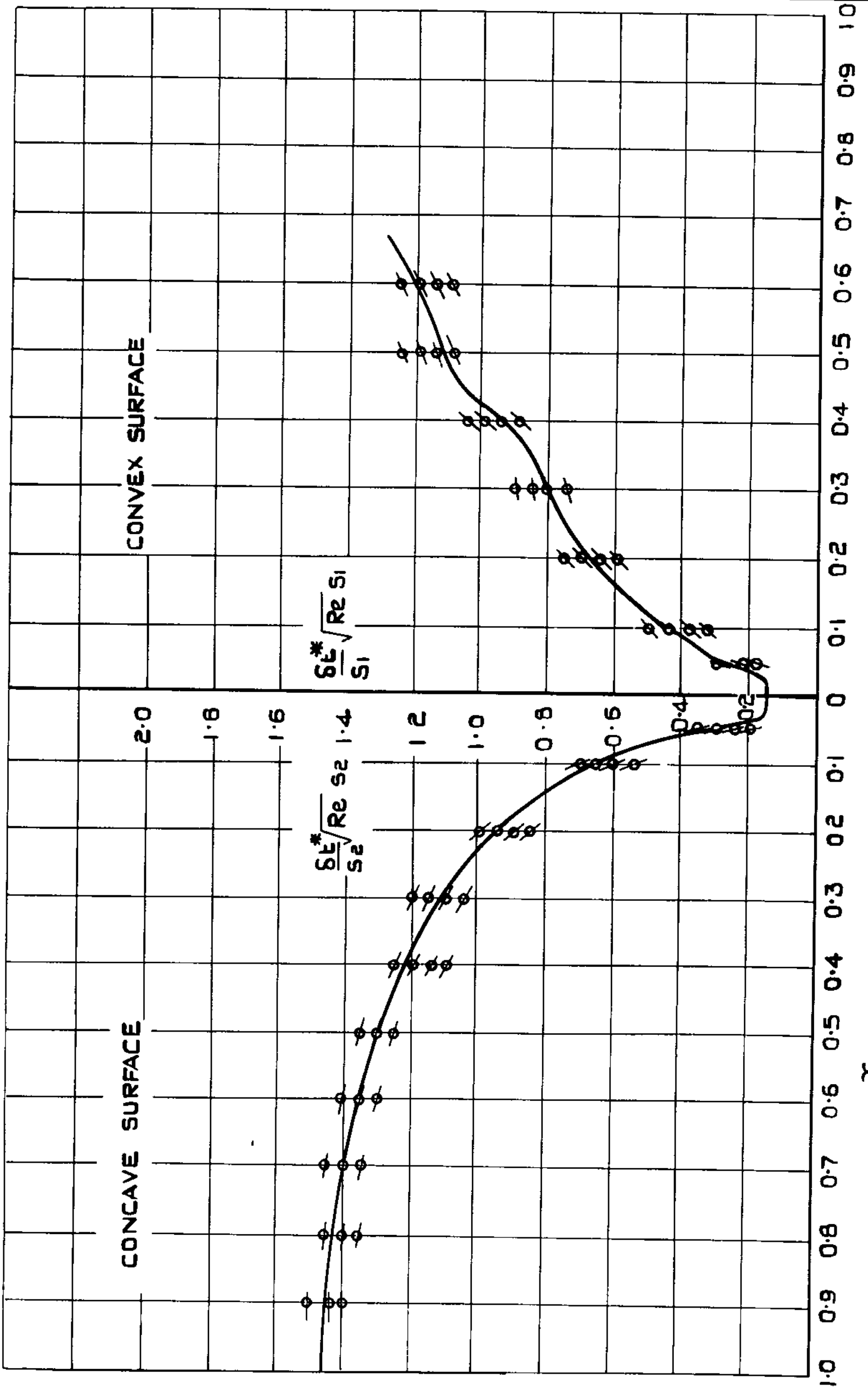


GRAPH OF $\frac{\delta t^*}{s_{1,2}}\sqrt{Re}$ AGAINST $\frac{x}{s_{1,2}}$ FOR THE W2/700 NOZZLE GUIDE VANE WITH NO INJECTION

FIG. 13

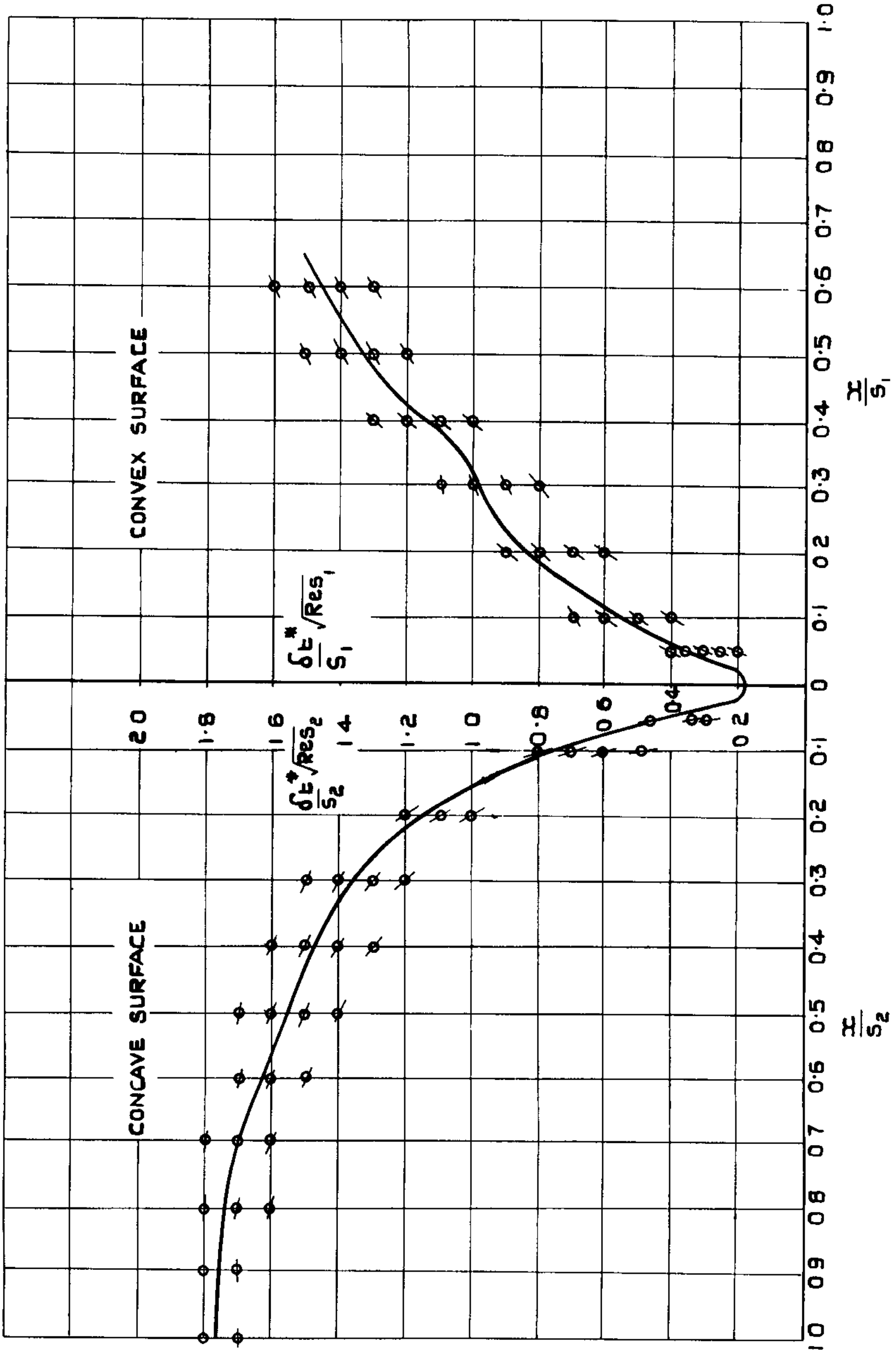


GRAPH OF $\frac{\delta t^*}{S_{1,2}}\sqrt{Re}$ AGAINST $\frac{x}{S_{1,2}}$ FOR THE W2/700 NOZZLE GUIDE VANE EFFUSION COOLED TO 600°C

NOTE ALL PHYSICAL CONSTANT AT FREE STREAM CONDITIONS

FIG.14.

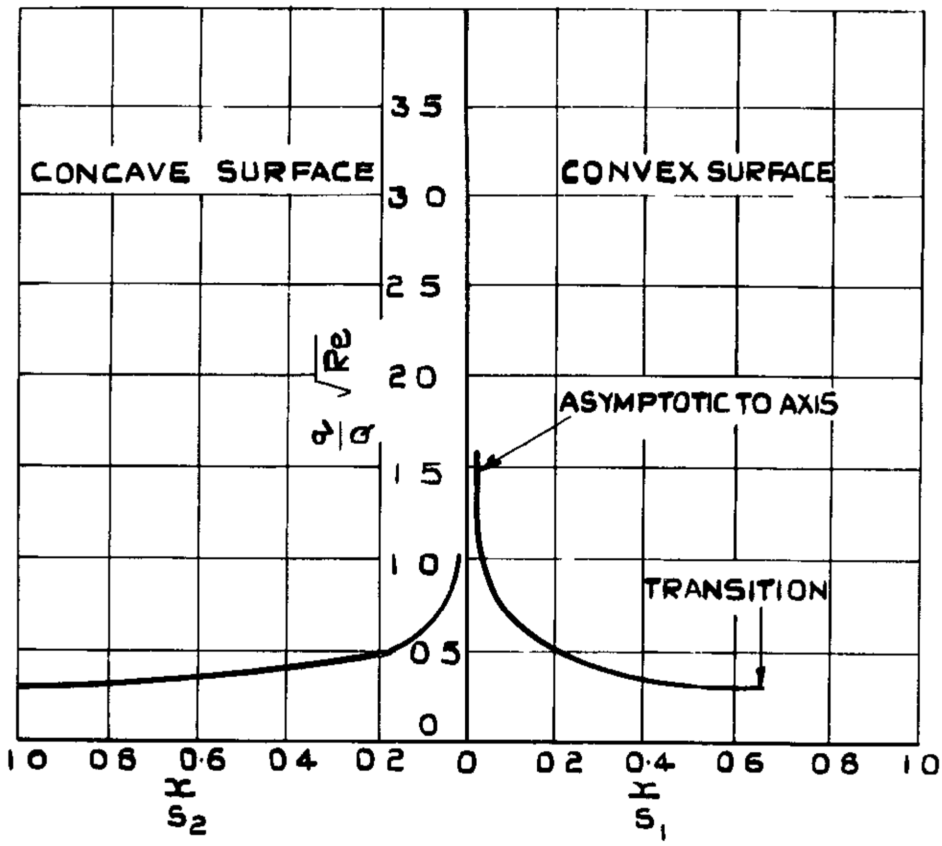


(a) COOLING AIR VELOCITY DISTRIBUTION REQUIRED TO COOL A NOZZLE GUIDE VANE TO 600°C IN A GAS STREAM AT 1,000°C (APPROX. SOLUTION)

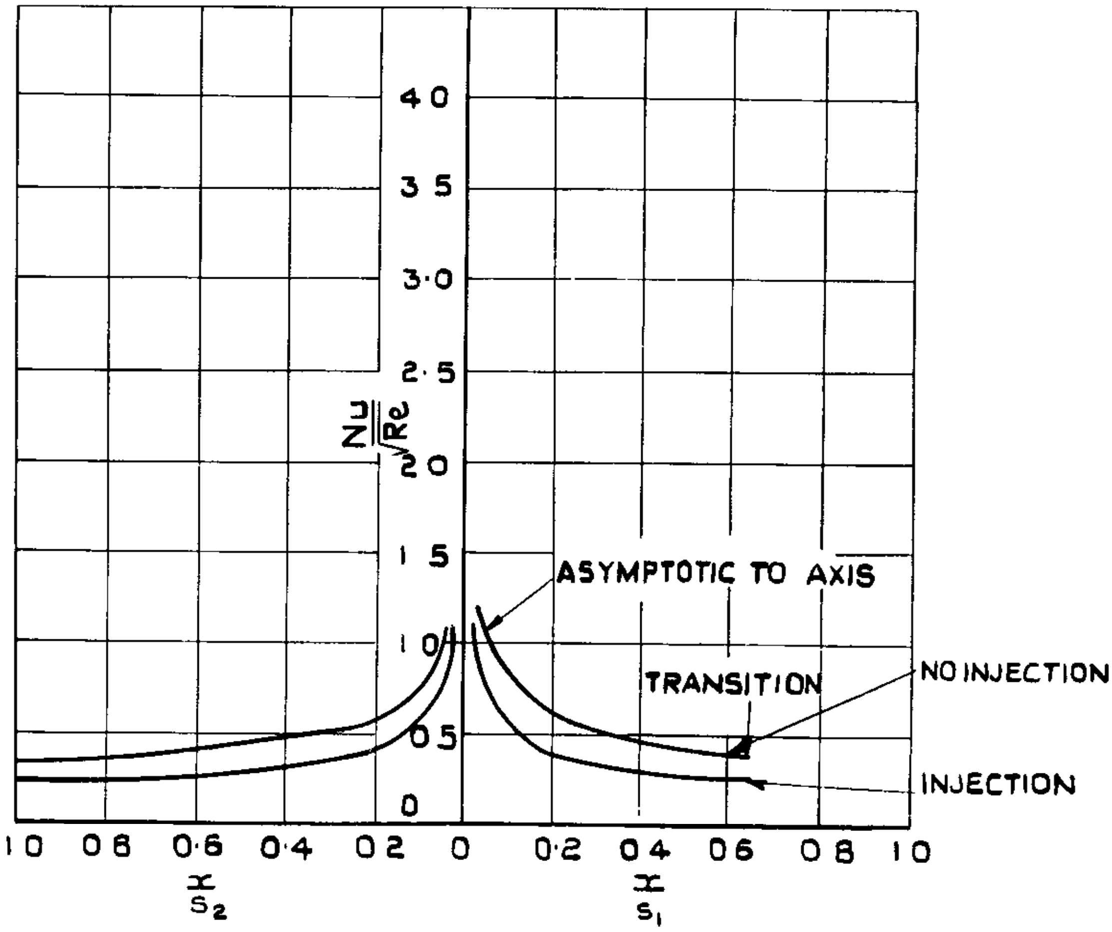


(b) COMPARISON OF HEAT TRANSFER WITH & WITHOUT INJECTION (APPROX. SOLUTION)

FIG. 15.

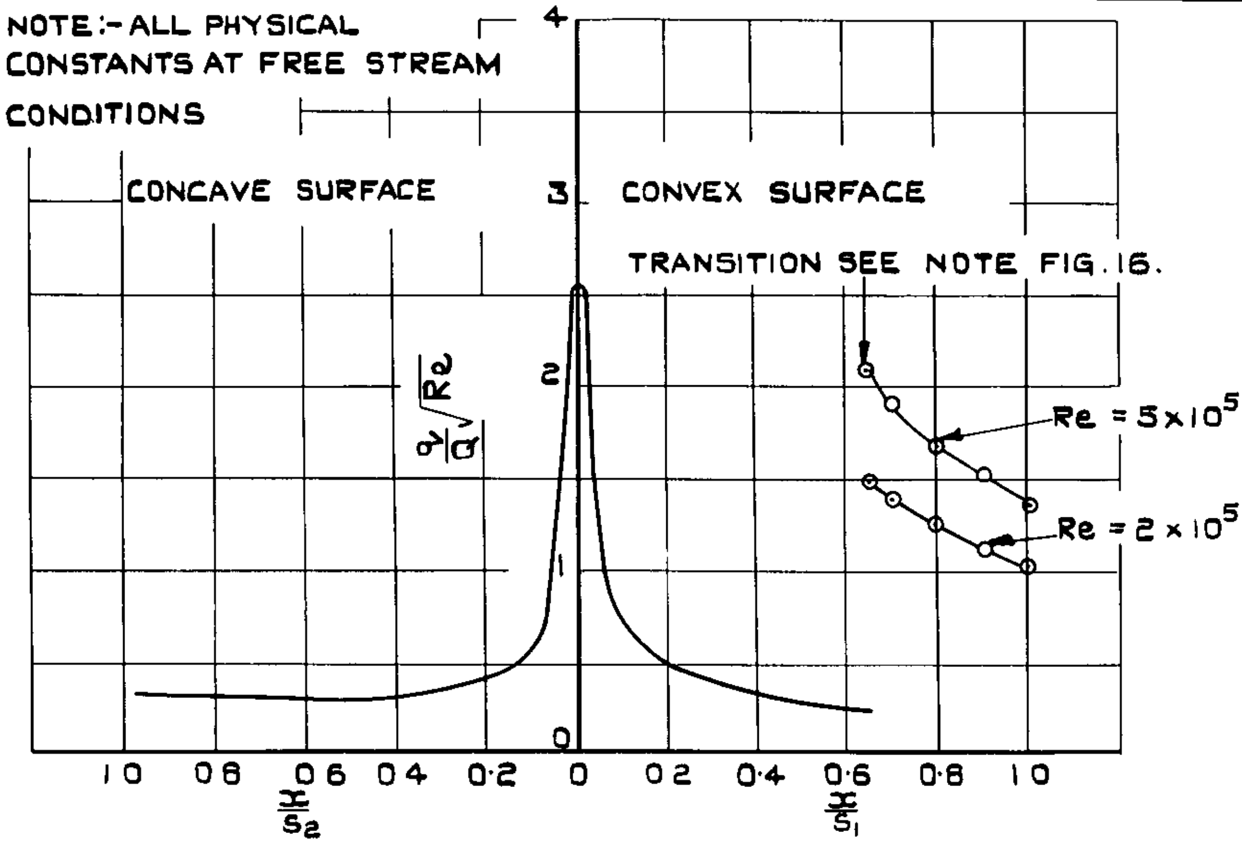


(a) COOLING AIR VELOCITY DISTRIBUTION REQUIRED TO COOL A NOZZLE GUIDE VANE TO 600°C IN A GAS STREAM OF 1000°C

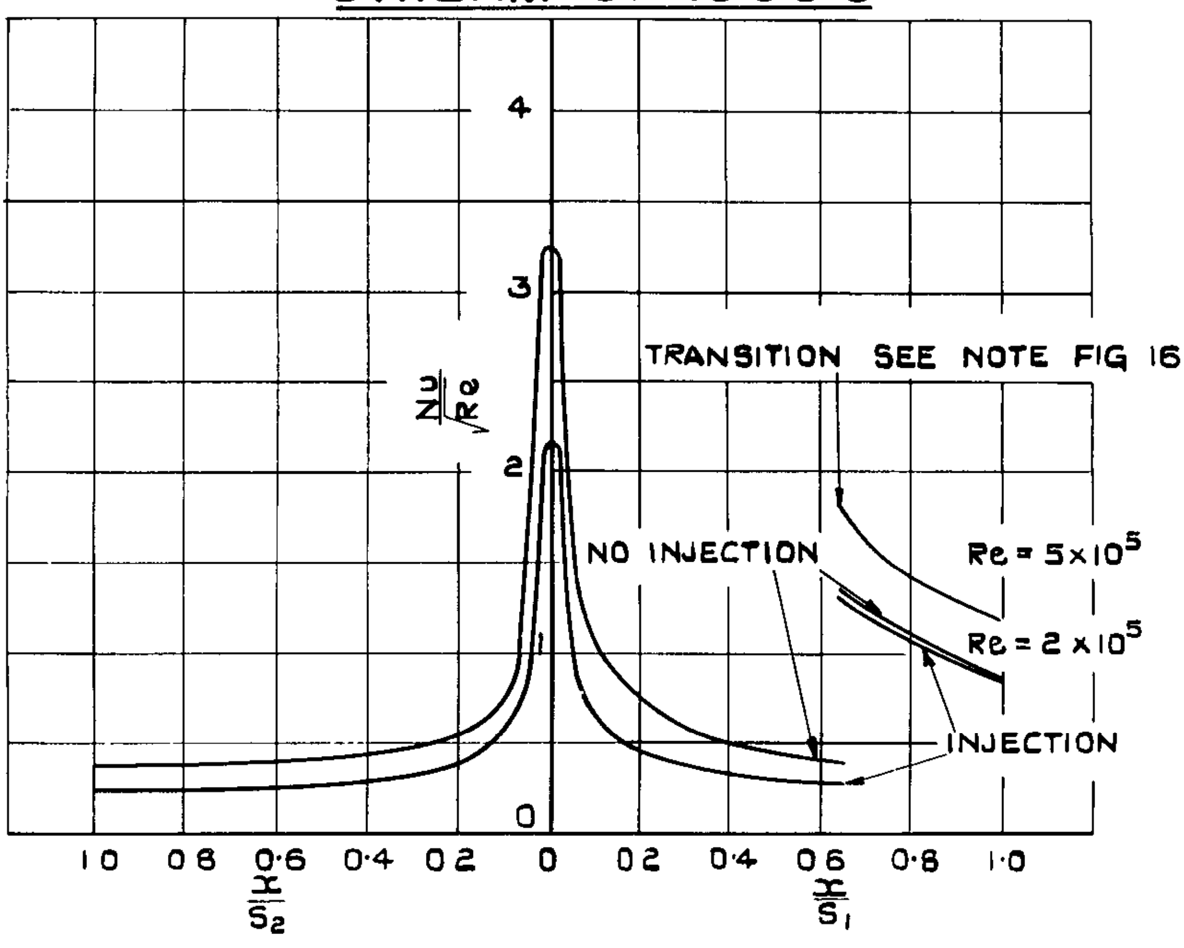


(b) COMPARISON OF HEAT TRANSFER WITH AND WITHOUT INJECTION

FIG.16.

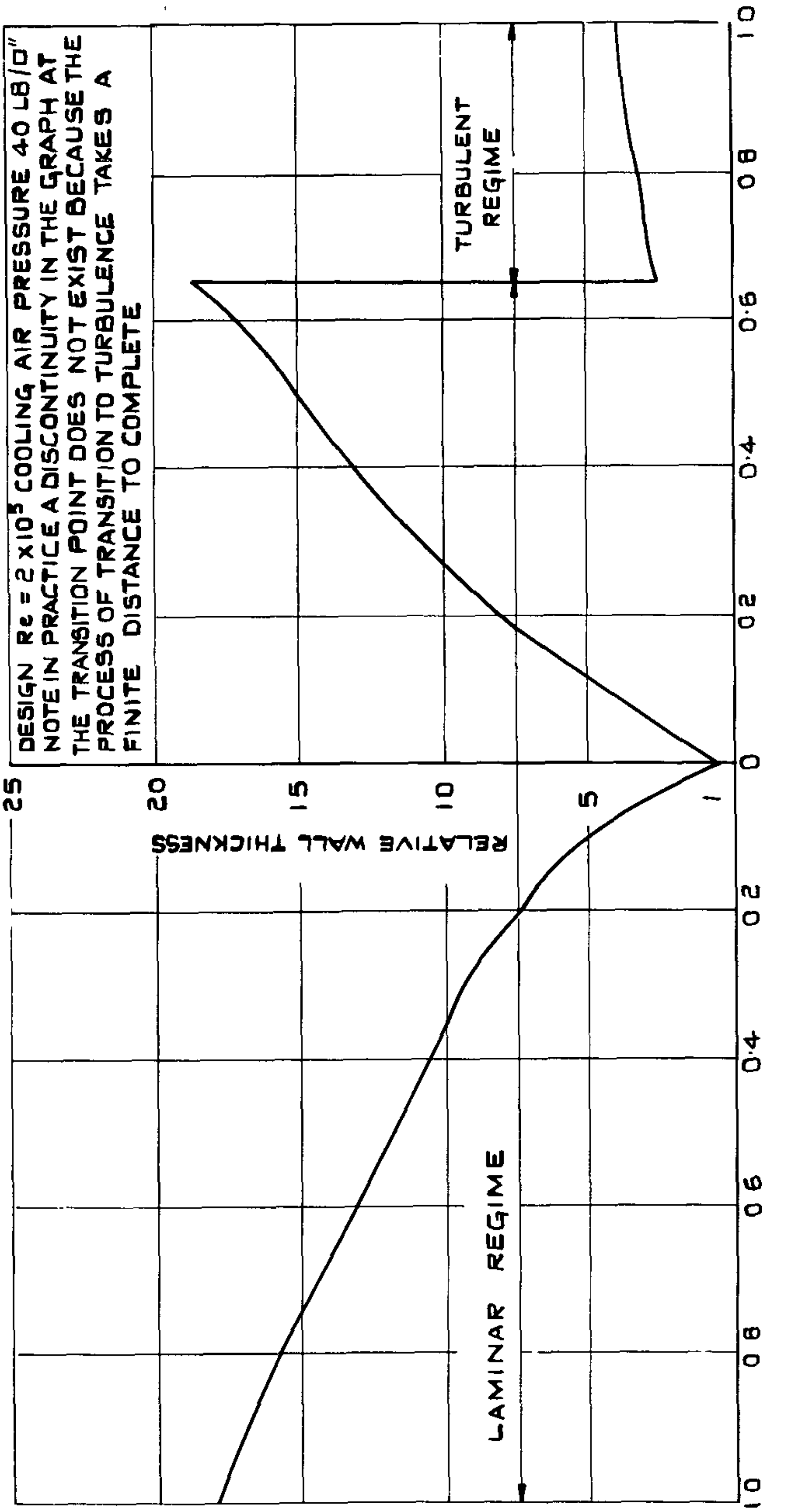


RELATIVE WALL THICKNESSES OF AN EFFUSION COOLED NOZZLE GUIDE VANE

FIG.17.

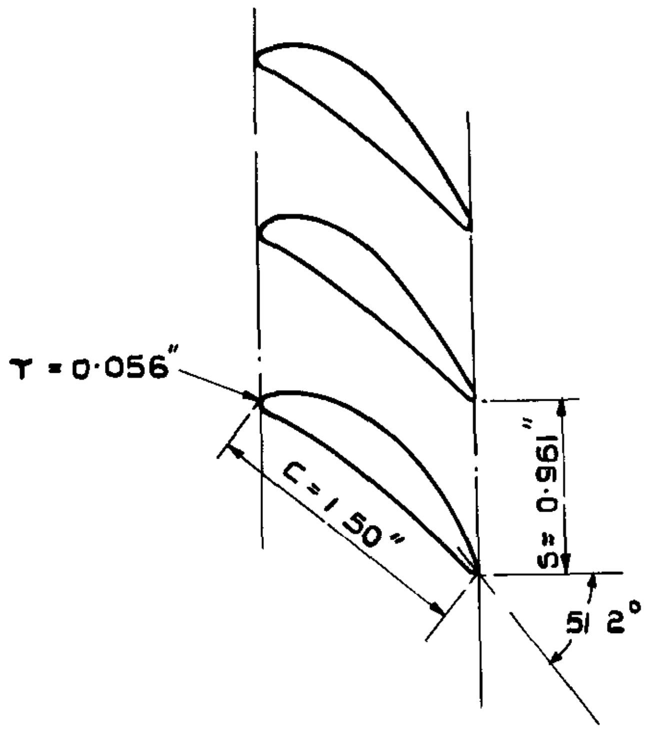


(a) DETAILS OF A NOZZLE CASCADE

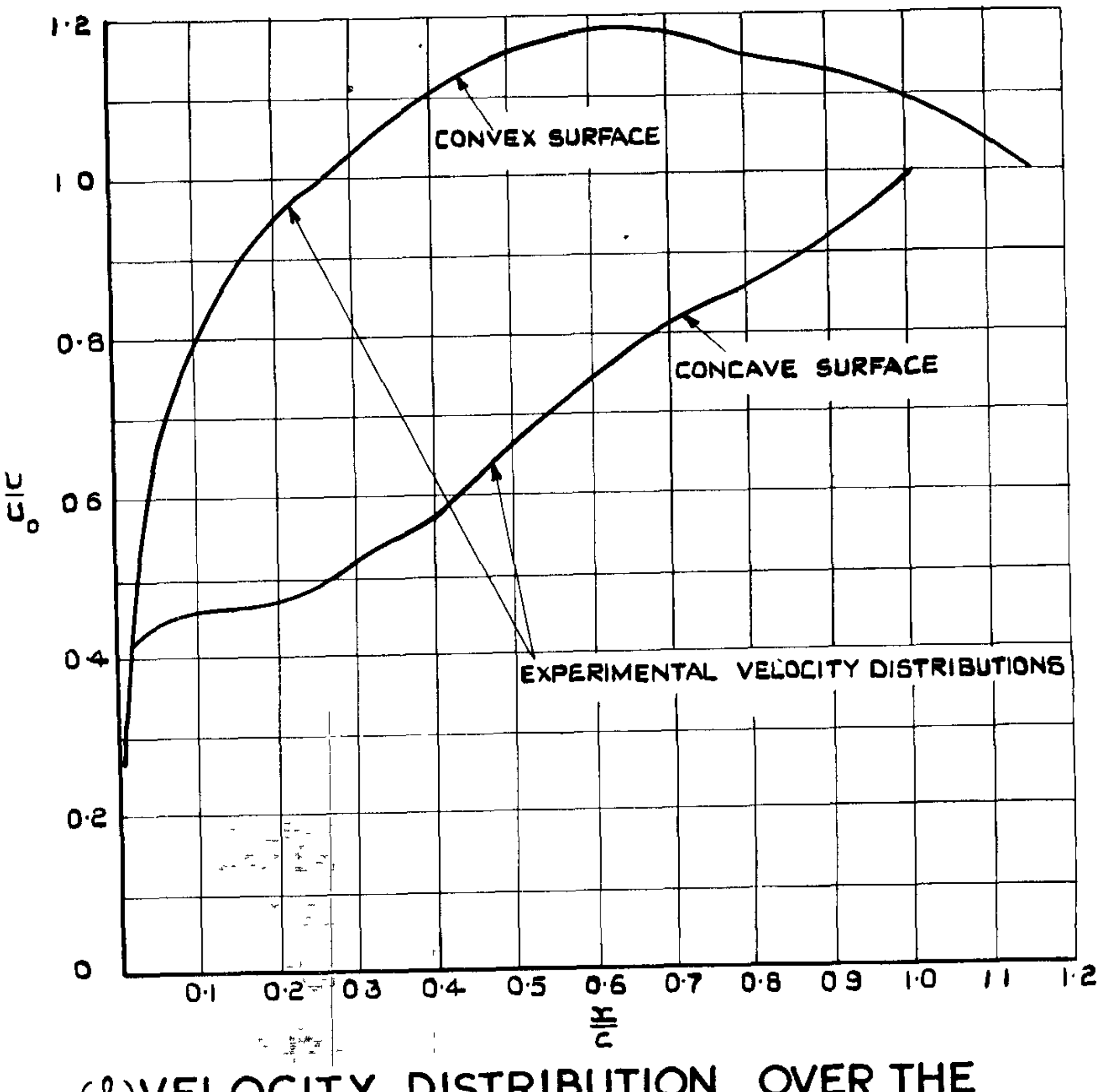


(b) VELOCITY DISTRIBUTION OVER THE SURFACE OF A NOZZLE BLADE

NOTE ALL PHYSICAL CONSTANTS AT FREE STREAM CONDITIONS.

FIG.18.

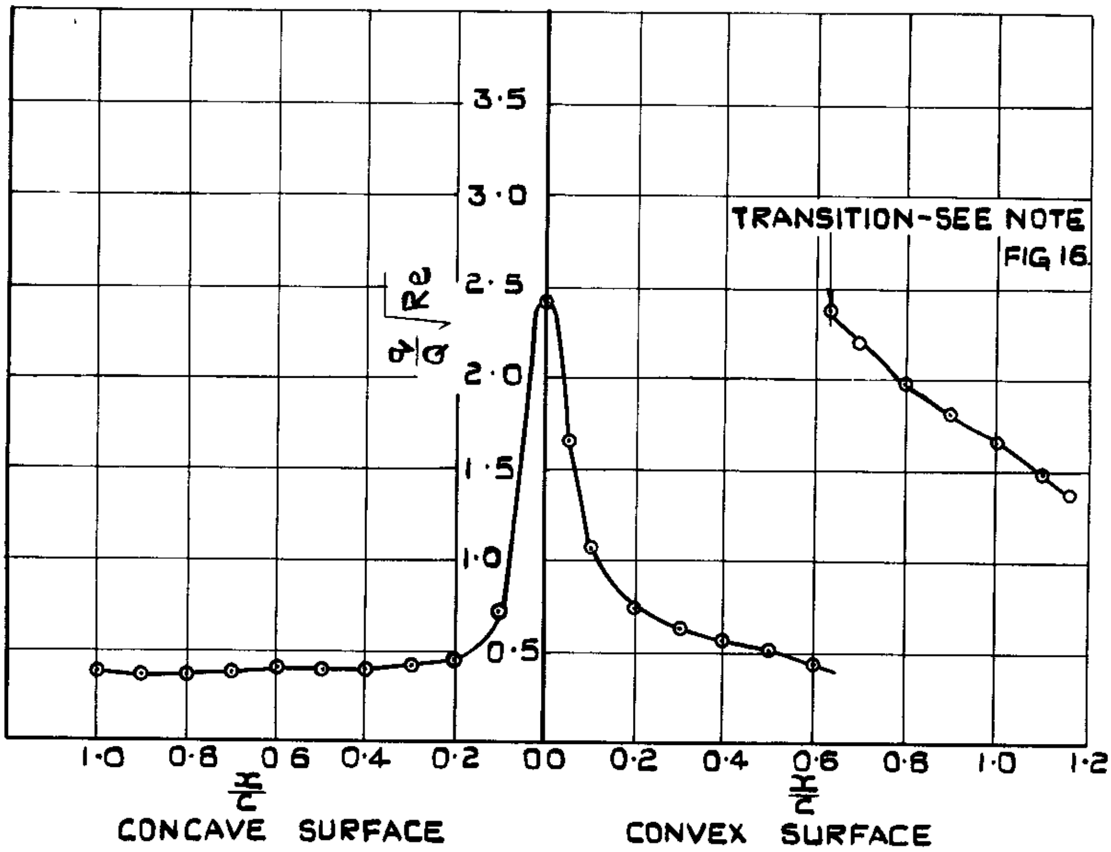


(a) COOLING AIR VELOCITY REQUIRED TO COOL A NOZZLE BLADE TO 600° IN A GAS STREAM AT 1200°C $Re = 2\times10^5$

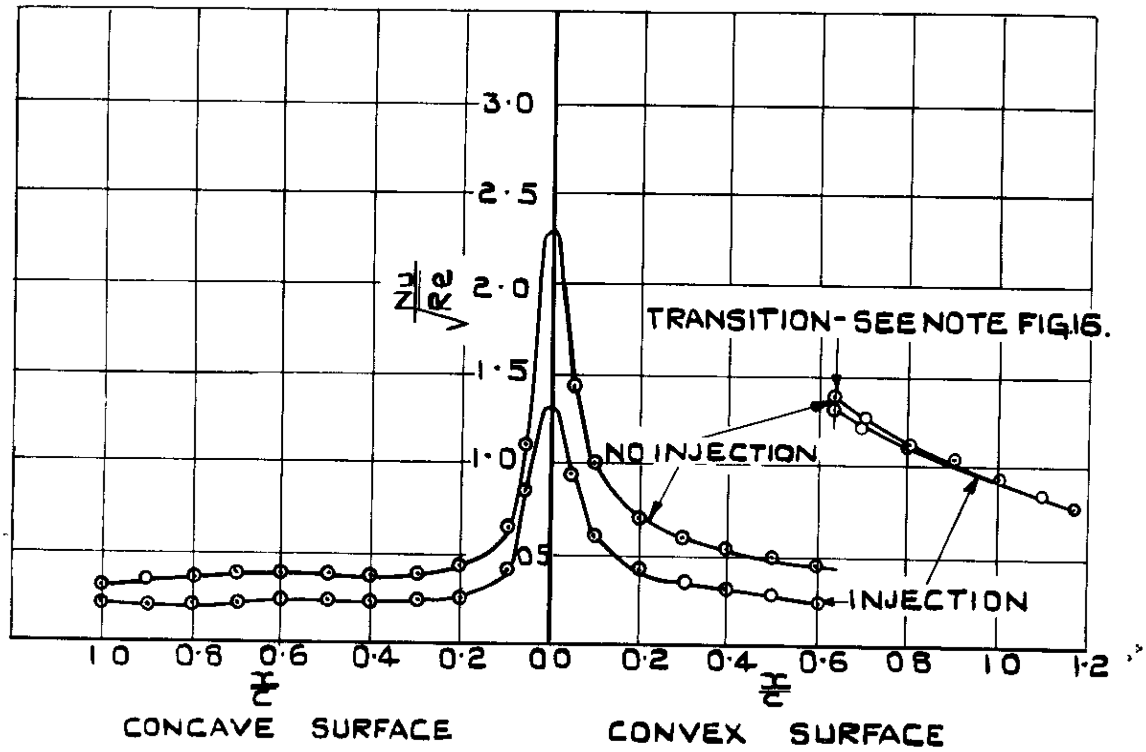


(b) COMPARISON OF HEAT TRANSFER WITH & WITHOUT INJECTION

FIG.19.

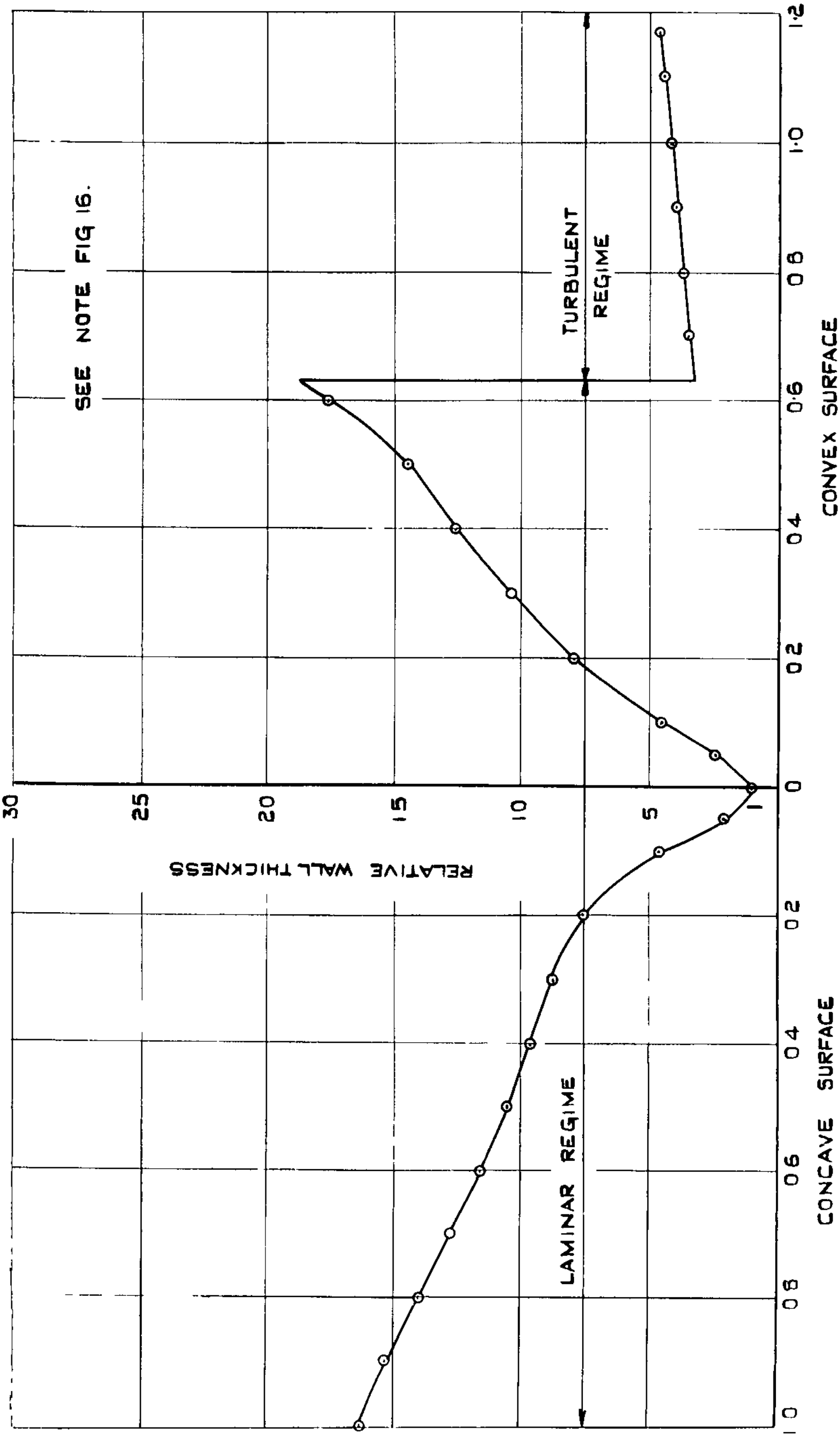


RELATIVE WALL THICKNESSES OF AN EFFUSION COOLED NOZZLE BLADE

C.P No. 165
(15,548)
A.R.C Technical Report



PRINTED AND PUBLISHED BY HER MAJESTY'S STATIONERY OFFICE
To be purchased from
York House, Kingsway, LONDON, W.C.2   423 Oxford Street, LONDON, W.1
P.O. Box 569, LONDON, S.E.1
13a Castle Street, EDINBURGH, 2   1 St. Andrew's Crescent, CARDIFF
39 King Street, MANCHESTER, 2   Tower Lane, BRISTOL, 1
2 Edmund Street, BIRMINGHAM, 3   80 Chichester Street, BELFAST
or from any Bookseller

1954

Price 4s 6d net

PRINTED IN GREAT BRITAIN

S.O. Code No. 23-9007-65